ADVANCED FUNCTIONAL MATERIALS
www.afm-journal.de

Liquid Metal-Based Biosensors: Fundamentals and Applications

Sina Jamalzadegan, Sooyoung Kim, Noor Mohammad, Harshita Koduri, Zach Hetzler, Giwon Lee, Michael D. Dickey, and Qingshan Wei**

Biosensors are analytical tools for monitoring various parameters related to living organisms, such as humans and plants. Liquid metals (LMs) have emerged as a promising new material for biosensing applications in recent years. LMs have attractive physical and chemical properties such as deformability, high thermal and electrical conductivity, low volatility, and low viscosity. LM-based biosensors represent a new strategy in biosensing particularly for wearable and real-time sensing. While early demonstrations of LM biosensors focus on monitoring physical parameters such as strain, motion, and temperature, recent examples show LM can be an excellent sensing material for biochemical and biomolecular detection as well. In this review, the recent progress of LM-based biosensors for personalized healthcare and disease monitoring via both physical and biochemical signaling is survey. It is started with a brief introduction of the fundamentals of biosensors and LMs, followed by a discussion of different mechanisms by which LM can transduce biological or physiological signals. Next, it is reviewed example LM-based biosensors that have been used in real biological systems, ranging from real-time on-skin physiological monitoring to target-specific biochemical detection. Finally, the challenges and future directions of LM-integrated biosensor platforms is discussed.

1. Introduction

Biosensors are detection tools that have been used for many applications such as disease diagnostics and health monitoring. One of the first biosensors was introduced in 1956 to detect O_2.[1] Over nearly 70 years, many studies have been conducted to enhance the analytical performance of biosensors, such as specificity, sensitivity, limit of detection (LOD), working range, and resolution.[2] Although biosensors have wide ranging applications, their use for healthcare is one of the major driving forces for the continuous improvement of sensor technology. For human applications, accurate, reproducible, low-cost, and biocompatible sensor technology is required for point-of-care (POC) and long-term use.[3]

In recent years, there has been increased interest in on-skin, wearable, and implantable sensors, which open tremendous opportunities for continuous and real-time monitoring of health metrics and bring a new horizon of digital health.[4] These types of sensors benefit from soft and stretchable electronics that enable sensors to attach to the human body and stretch in concert with body movements.

Current wearable sensors are mainly based on polymer and nanomaterials to form the stretchable substrates and active sensing materials, respectively. Flexibility and biocompatibility are the two important factors of sensor substrate selection for wearable applications.[5] Polydimethylsiloxane (PDMS), polyethylene terephthalate (PET), polyurethane (PU), and EcoFlex are the most widely used substrates for soft sensor fabrication.[6] In addition, the selection of deformable sensing materials is also essential to enhance the performance of the wearable sensors. Frequently, carbon-based materials like carbon nanotubes (CNT) and graphene, as well as gold, copper, and silver nanomaterials were frequently used as active sensing elements.[7,8] Although these types of materials showed high conductivity properties, they have mismatched mechanical properties when compared to the substrates and could not be stretched freely.[9]

Compared to the commonly used active sensing materials for wearable sensors, such as metallic nanomaterials and their composites,[10] liquid metals (LMs) on the other hand are inherently soft and can form elastic conductors by encasing them in elastomer. LMs uniquely combine physical and chemical features of liquids and metals, such as fluidity, high thermal and electrical conductivity, low vapor pressure, good deformability, low melting point, and high surface tension.[11] They have been utilized for sensing pressure, strain,

S. Jamalzadegan, S. Kim, N. Mohammad, H. Koduri, Z. Hetzler, G. Lee, M. D. Dickey, Q. Wei
Department of Chemical and Biomolecular Engineering
North Carolina State University
Raleigh, NC 27695, USA
E-mail: mddickey@ncsu.edu; qwei3@ncsu.edu
G. Lee
Department of Chemical Engineering
Kwangwoon University
Seoul 01897, Republic of Korea

The ORCID identification number(s) for the author(s) of this article can be found under https://doi.org/10.1002/adfm.202308173

DOI: 10.1002/adfm.202308173

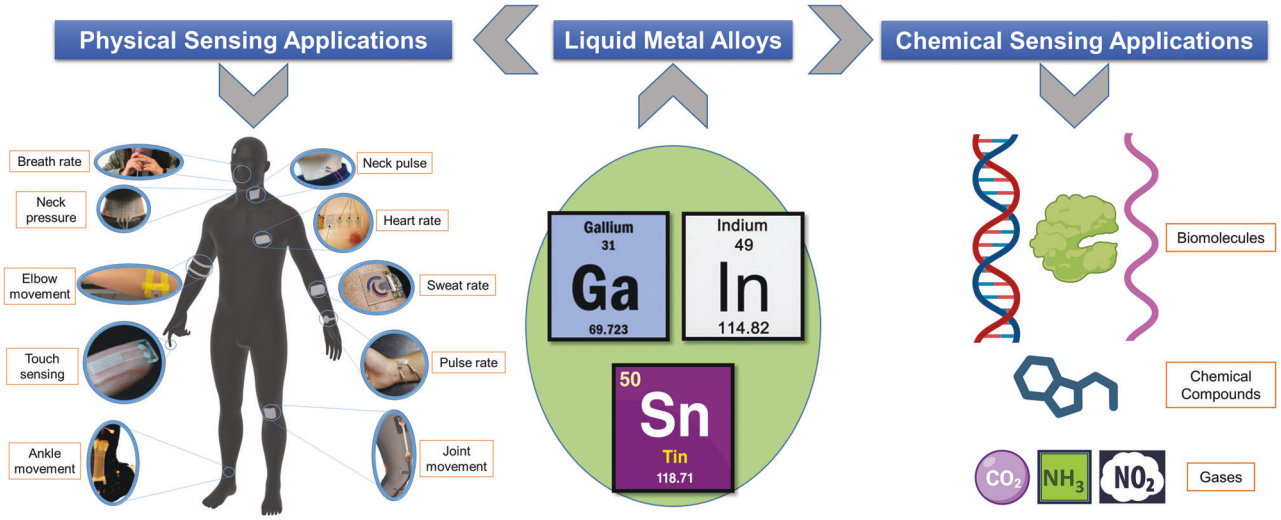

Scheme 1. Summary of properties, sensing mechanisms, and applications of liquid metal-based biosensors in physical and chemical biosensing.

force, biomolecules, and chemicals.[12] Gallium (Ga) and mercury (Hg) are metals with melting points below body temperature. Since the toxicity of Hg is a great concern,[13] Ga and its alloys have been more widely explored in the biosensor field.[14,15]

In this review, we provide an overview of the state-of-the-art LM-based biosensors, with a particular emphasis on applications related to monitoring health metrics and diagnosing disease. For the general applications of LMs for sensors, there are several other recent review articles to which the readers can refer.[12,16–19] In this work, we start with a brief introduction of the basics of biosensors and LMs. Then, we summarize the different LM-based biosensor mechanisms in detail and highlight the recent applications of LM-integrated biosensors for healthcare applications, ranging from on-skin monitoring to biomarker detection (**Scheme 1**). Finally, we discuss the challenges and future prospective opportunities that LMs could bring for next-generation sensor devices. Regarding the fabrication and miniaturization of devices containing liquid metal, we point the reader to a recent review.[20]

2. The Need for Soft Biosensors

Biosensors are often used to measure either physiological signals (e.g., heart rate, body temperature) or biomarkers (i.e., molecules from the body that provide information about health status). Biomarkers include nucleic acids,[21–24] enzymes,[25] exosomes,[26] and cells[26,27] that can be derived from various biofluids like blood, sweat, and tears.[28] In addition, the ability to sense small molecules such as volatile organic compounds (VOCs) is useful for noninvasive detection of human[29] or plant diseases.[30–34] Sensors convert the presence of biomolecules into a measurable/detectable signal.[17] An important challenge is to make the sensor specific to target molecules, which is typically achieved by introducing bio-specific ligands or biorecognition elements into the sensor interface. Signals generated by biorecognition events are then sensed by a chemical or physical transducer, transmitted, and amplified if needed.[17] For signal transduction, several mechanisms are commonly used, including fluorescent,[21,22,35] colorimetric,[36] electrical,[37] size-based,[38] and surface plasmon resonance modalities.[28] In addition to biomarkers, biosensors can also measure biophysical parameters like temperature,[39] sound,[17] light,[40] and force.[41] Biosensors have been widely applied to monitor the health and status of humans, the environment, agriculture, and food.[17]

While most existing biosensors are rigid, the need for soft, stretchable sensors are increasing. Soft biosensors use materials whose mechanical properties are similar to the body for several reasons, and attract tremendous attentions due to the following reasons: First, they are more comfortable to wear or lead to less scaring for implantable devices that interface tissue. Second, conformal biosensor is able to acquire time-resolved host body biomatrices via direct contact and continuous monitoring. Third, soft biosensors have built in stress release designs which can reduce issues associated with reproducibility of rigid biosensors arising from deformation.[42] Fourth, soft biosensors can utilize geometric deformation to perform sensing or generate power, which opens new application possibilities.

Liquid metals (LMs), especially Ga, are drawing great attention for biosensors because of their unique physical and chemical properties, such as stretchability and conductivity. The stretchability of LMs makes them ideal for developing soft electrodes,[43,44] antennas, and electrical interconnects[45] for biosensor fabrication. LM-based soft electrical circuits adopt the mechanical properties of the encasing material, allowing for the formation of very soft and stretchable conductors.[46] Unlike traditional solid circuits, which are often fabricated using lithography, LM can be patterned in new ways such as injection, printing, or direct writing.[20] These methods are convenient and easy to implement.[47] LM has been demonstrated for implantable electrodes for sensing biomolecules inside the body.[45] Indeed, many LM-based sensors have been recently demonstrated to sense a wide range of targets such as temperature,[39] pressure,[48] force,[49,50] gas molecules,[51–58] ions,[59,60] and biomolecules.[43,45,61]

Table 1. Physical properties of Ga-based liquid metals.[64]

Property	Ga	EGaIn	EGaInSn
Viscosity (Pa s)	1.4×10^{-3}	2.0×10^{-3}	2.4×10^{-3}
Specific heat (J kg^{-1} K^{-1})	4.1×10^{2}	4.0×10^{2}	3.0×10^{2}
Thermal conductivity (W m^{-1} K^{-1})	2.9×10	2.7×10	2.5×10
Electrical conductivity (S m^{-1})	6.7×10^{6}	3.4×10^{6}	3.3×10^{6}
Melting point (°C)	29.8	15.5	11

3. Fundamentals of Liquid Metals

3.1. Liquid Metals and Their Alloy Composition

Liquid metals are metals or metal alloys which are liquid at or near room temperature. Ga has low toxicity,[62] which makes it more appealing for biosensor applications than Hg. The melting point temperature of Ga is 30 °C. Thus, at room temperature, it is solid, although it can also exist as a liquid due to its ability to supercool.[63] The melting point temperature decreases when introducing other metals to Ga to form alloys, such as indium (In) for making eutectic Ga-In (EGaIn, with a composition of Ga 75.5 wt% and In 24.5 wt%, melting point 15 °C) and tin (Sn) for forming eutectic Ga-In-Sn (with a composition of Ga 68.5 wt%, In 21.5 wt%, and Sn 10 wt%, melting point 11 °C).[64] Except for the melting point, Ga and most Ga-based liquid metal alloys have similar properties, such as viscosity, specific heat, and thermal and electrical conductivity[65] (**Table 1**). Therefore, to a first approximation, these liquids can be used interchangeably for many applications. In addition to bulk liquid metal, liquid metal composites can be made by mixing liquid metals with other materials such as metal particles and polymers.[66,67] Recent reviews highlight various liquid metal composites that have been prepared.[68,69]

3.2. Physical and Chemical Properties of Liquid Metals

LMs uniquely have both metallic and liquid properties, which is useful for creating soft conductors[70] and enabling new methods to pattern metallic materials.[20] Importantly, Ga has extremely low vapor pressure. It is measured as 1.5×10^{-7} atm at 1170 °C and estimated thermodynamically as 10^{-44} atm at room temperature,[65,71] unlike Hg[65,72] (1 Pa at room temperature), which makes it possible to handle Ga-based LMs outside of a hood without concern for breathing metallic vapor. It also means that devices that use Ga-based LMs will not lose material over time via evaporation.

Gallium is also considered to have low toxicity and has been used in laboratory examples on human skin[73] or for drug delivery.[74] Several Ga compounds (e.g., salts) have been Food and Drug Administration (FDA) approved for applications such as serving as diagnostic and therapeutic agents.[75] Due to similarities between Ga^{3+} (the favored oxidation state) and Fe^{3+}, a similar mechanism may occur to remove Ga^{3+} from the body. Nevertheless, careful handling of LM is recommended. Certain types of Ga complexes known as gallium halide with chalcogenide complexes in 4-methylpyridine are toxic.[76] While these require special synthesis and thus are not found in any of the sensors described herein, this example is a reminder of using caution with new materials. Furthermore, mechanical agitation such as sonicating LM in water increases the concentration of Ga^{3+} and In^{3+} in solution. After sonication, the concentration of In^{3+} ions would be drastically increased and become of the same magnitude as the concentration of Ga^{3+} ions. Combined, those ions were found to kill cells after 3 days.[77] Thus, while many studies indicate liquid Ga has low toxicity, more studies should be conducted to better understand the biocompatibility.

In the presence of oxygen, Ga-based LMs form a very thin oxide layer, which is often called an "oxide skin". It is ≈3-nm thick and forms rapidly, even in environments with more than 1 parts per million (ppm) oxygen.[78] The oxide layer can be removed simply by applying electrical potential[79,80] or by dissolution using strong acid/base solutions[81–83] since the oxide layer is amphoteric.[70] The oxide is considered to be amorphous Ga_2O_3, but it can convert to GaOOH in the presence of water.[84] The presence of the oxide layer allows LM droplets to form non-spherical shapes and stick to most untreated surfaces despite the large surface tension of the bare metal.[85] In addition, dispersion of other particles into LMs can be challenging due to their immiscibility, but the native oxide layer can help enable dispersion by encasing the particles and preventing their agglomeration.[86]

3.3. Device Fabrication and Applications in Soft Electronics

Because of their fluidity and high electrical conductivity, LMs are excellent candidates for soft electronics.[70] Here, we highlight a few illustrative examples that showcase the unique properties of LM while pointing the reader to more comprehensive reviews highlighting the promising applications of LMs in soft electronics.[70,88] As metallic conductors, LMs can be used for interconnects, antennas, and electrodes. They are also easy to pattern in unique ways. LM patterning and fabrication involve various techniques, including injection filling into microchannels and 3D printed cavities, as well as direct ink writing through methods like inkjet printing and extrusion 3D printing (**Figure 1a–c**). For example, LMs can be filled in microfluidic channels via direct injection or vacuum filling[89,90] (Figure 1a). These channels filled with LM can function as stretchable circuits if the encasing material is elastomeric [91] (Figure 1d). When a part of the LM circuit is cut, the exposed LM immediately forms an oxide layer that prevents leakage. When the two cut planes come together, the electrical connection will reform.[92,93] Thus, they can form self-healing circuits and textiles (i.e., that can retain conductivity after being cut or damaged).[92,94–96] Stencil-based patterning, utilizing the fluidity of LM and its oxide's adherence, is an another popular and automated approach, while selective wetting on smooth surfaces and rheological modification for controlled shaping further contribute to the versatility of LM fabrication methods.[87] Printing liquids into 3D structures is challenging due to the tendency of liquids to flow and minimize surface energy.[100] However, the solid oxide skin makes the printing of LM possible. For example, if two droplets of LM come into contact, they will not completely merge into a single droplet; thus, it is possible to 3D print

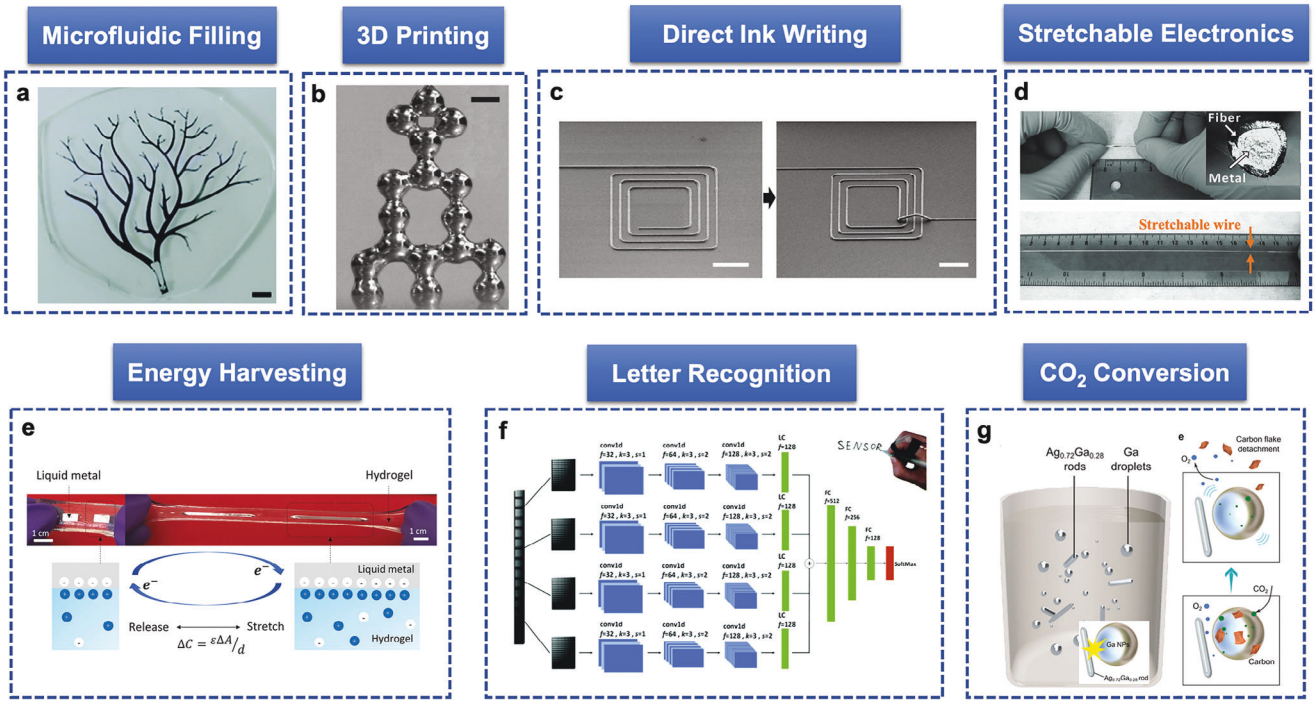

Figure 1. Patterning and recent applications of LMs. a) Silicone microchannels filled with LM by vacuum filling[90] (Scale bar, 5 mm). Copyright 2017, The Royal Society of Chemistry. b) A self-supporting LM tower made by stacking liquid metal droplets.[101] Copyright 2013, Wiley-VCH GmbH. c) 3D-printed LM lines[103] (Scale bars, 200 μm). Copyright 2019, AAAS. d) The top image is an ultrastretchable conductive LM fiber before being stretched (2 cm). The inset is the cross-section image of the fiber with an LM core and elastomer shell. The bottom image is the stretched fiber to 20 cm.[91] Copyright 2013, Wiley-VCH GmbH. e) A photograph of an LM-based energy harvester (top). The LM electrodes are encased by hydrogel. The bottom image shows the schematic of energy harvesting principle.[98] Copyright 2021, Wiley-VCH GmbH. f) EGaIn-hydrogel strain sensor integrated with convolutional neural network for letter recognition during writing.[104] Copyright 2022, The Royal Society of Chemistry. g) Ga particle-based CO_2 conversion.[105] Copyright 2021, Wiley-VCH GmbH.

LM[101] (Figure 1b). Furthermore, LM can be printed via direct writing because the oxide layer adheres to surfaces strongly[102,103] (Figure 1c).

LMs have been used to create soft devices for various applications such as energy harvesting, which may be useful for powering wearable sensors. For example, they can be used as highly conductive and stretchable wiring for thermoelectric devices that convert thermal energy (e.g., from the skin) into electricity.[97] As another example, varying the area of the electrical-double-layer (EDL) that forms between LM and hydrogel can convert mechanical energy to electricity[98] (Figure 1e). Stretching the hydrogel that encases LM deforms the LM and thereby increases its interfacial area (ΔA) with the hydrogel. The increased area, and thus, capacitance (C), of the EDL drives the movement of charge through an external circuit. Releasing the hydrogel causes charge to flow in the opposite direction. Attaching these soft devices to the body can enable the conversion of body motion to electricity.[99]

The metal can also be used for strain sensing to detect letter recognition by using the pressure signals of a single handwritten letter as an input and conventional neural network to classify the data and recognize written words as the output (for example the word "sensor" in this research)[104] (Figure 1f). Liquid metal can also drive chemical reactions. For example, mechanical stirring can convert dissolved CO_2 into solid C[105] (Figure 1g). It is thought that the stirring causes LM particles and intermetallic nanorods of Ag Ga to bump into each other, resulting in tribocharging that drives the reaction. This work is exciting because it uses only mechanical energy to reduce CO_2 and produces easy-to-store solid C that exfoliates from the metal surface. Beyond these aforementioned uses of LM, applications of LM in biosensing area are emerging as summarized in this review.

4. Transducing Mechanisms of Liquid Metals

Both bulk LMs and LM-based nanoparticles have been used to transduce biochemical or physiological inputs from the body into electrical, optical, and magnetic signals for sensing (**Table 2**). Among them, changes in resistivity, capacitance, and electromagnetic properties, are the main mechanisms of sensing in the past fifteen years.[17,106] These changes can arise, for example, due to changes in geometry of LM in response to force (pressure, touch, shear, elongation).[107] Because LM is a liquid, it is very easy to deform in response to force. The sensitivity can be enhanced further based on the design of the geometry.[17] In addition to sensing changes to resistance and capacitance, piezoelectric,[108–110] inductive,[111–114] electrochemical,[59,115] and optical[58,116,117] sensing have also been demonstrated using LMs. This section summarizes the various transduction mechanisms that use LM.

Table 2. Advantages and limitations of different LM-based transduction mechanisms.

Transduction Category	Sensing Capabilities	Advantages	Limitations
Electrical (ΔR, ΔC, V, I)	Strain Pressure Potential	High thermal and electrical conductivity Excellent stretchability and softness[159] High sensitivity Fast response Directly responsive to physical stimuli (touch, strain, and compression)	Signal interference due to mechanical perturbation Pattern resolution (10–100 µm common, yet ≈100 nm structures are possible)[160]
Electrochemical	Molecules Ions	High conductivity Considerable reduction potential for Ga and In ions Straightforward surface functionalizing	Reactivity of LM & native oxide Electrode fouling[161]
Optical (Plasmon, diffraction)	Strain Molecules	Localized surface plasmonic effects [148] Plasmonic coupling	Surface plasmon resonance (SPR) absorption mainly in the UV region for 200 nm diameter EGaIn Nanoparticles[147]
Magnetic	Strain Pressure	Low-cost and easy LM composite fabrication,[162] Useful for remote control sensing[163]	Pure Ga is weakly diamagnetic[12]

4.1. Electrical LM Transducer

The most prevalent sensing mechanism for liquid metal is based on electrical signals, which includes capacitive, resistive, and electrochemical transducers.

4.1.1. Capacitive Transducer

There are three modes of capacitive sensing: 1) self-capacitance, 2) mutual capacitance, and 3) deformable capacitors. The first two categories are useful for measuring the presence of the gentle touch of a finger, such as the sensors found on commercial touch screens. Self-capacitance measures changes in the capacitance of a single electrode or conductive surface. As an example, LM wires encased in a thin layer of elastomer can sense light touch via changes in self-capacitance without the need to physically deform the wire.[118] Mutual capacitance senses changes in capacitance between two electrodes. The presence of a dielectric (e.g., a finger) in close proximity disrupts the field lines between the electrodes and thereby changes the capacitance.[119] In principle, self- and mutual-capacitance sensors do not require soft materials, although using stretchable materials is nevertheless attractive for enabling comfortable devices. In contrast, a deformable capacitor requires soft materials and is therefore a compelling sensor for using liquid metal.

Equation (1) shows that the capacitance (C) depends on the dielectric constant (ϵ_r), distance between electrodes (d), and relative area between electrodes (A). ϵ_0 is the dielectric constant for the vacuum of the dielectric layer. By building a deformable capacitor from soft materials, it is possible to vary the geometry (typically d) of the capacitor in response to deformation.

$$C = \frac{\epsilon_0 \epsilon_r A}{d} \tag{1}$$

Capacitive sensors typically increase capacitance in response to force by decreasing the distance, d, between the electrodes. Equation (2) determines the sensitivity in response to exerted pressure.

$$\text{Sensitivity} = \frac{(C - C_i)}{C_i (P - P_i)} \tag{2}$$

where C is the capacitance of the capacitor at strain of ϵ; C_i is the initial capacitance; P is the applied pressure; and P_i is the initial pressure. The drawback of this equation is that it can result in division by zero or extremely small values when denominator approach zero. This leads to unreliable and potentially meaningless sensitivity calculations. To solve this issue, regularization or smoothing techniques can be applied by adding a small constant to the denominator, preventing division by zero or near-zero values.[120,121]

Based on equation (2), the sensitivity can be enhanced by designs that result in large changes in capacitance in response to small forces. To enhance the sensitivity, some strategies have been applied: 1) Using soft or porous dielectric layers, 2) increasing the dielectric constant, and 3) introducing microstructures in the dielectric layer.[122] We will discuss each of these in the following paragraph.

Minimizing the modulus of the dielectric layer maximizes the amount of geometric deformation in response to force; that is, d decreases, and thus, C increases. For this reason, PDMS and PU are common elastomeric dielectrics. PDMS is one of the most popular choices due to its low modulus, biocompatibility, ease of processing (it can be formulated as a liquid and cured into a solid), and chemical stability.[123,124] Porous dielectric layers can further decrease the effective Young's modulus and thereby increase sensitivity to deformation. Pores decrease the initial capacitance (C_i) since air is a poor dielectric. Deformation can displace the air and collapse the pores, thereby increasing the effective dielectric constant and thus C (Equation 2). It is also possible to make the dielectric soft by structuring it. For example, arrays of pyramids may be used for the dielectric layer with a working principle similar to the foams. The increase in the effective dielectric constant in response to deformations called positive piezopermittivity (piezo for touch).[121,122] It is possible to create negative

piezopermittivity by using fillers of LM particles in the elastomer; the fillers change shape during deformation, causing a decrease in the effective permittivity. Negative piezopermittivity is less useful for sensing, but can be used for capacitors that do not change capacitance with deformation.[121]

Capacitive LM sensors are widely applied for detecting pressure[118,125,126] resulting from touch or mechanical disturbance normal to the surface of the capacitor or strain applied in-plane. In this latter case, LM is particularly attractive as an electrode because it is easy to stretch. When the elastomer containing LM is stretched, the effective area of the electrodes increases, which effectively decreases the distance between them. This combination of factors results in an increase in the capacitance of the capacitor.[127]

Measuring strain via capacitive sensors requires calibrating the relationship between deformation and capacitance. Liquid metals are attractive as electrodes because 1) they effectively do not contribute to the overall mechanical stiffness (that is, a device constructed of silicone will have, to a first approximation, silicone-like mechanical properties), and 2) they can conform to the dielectric materials during deformation.

4.1.2. Electrical-Double-Layer Capacitor Transducer

An electrical-double-layer capacitor sensor (EDLC) can sense changes in capacitance between an electrode and electrolyte. Electrical double layers form spontaneously at the interface between an electrode and electrolyte, such as that formed between LM and hydrogel. The amount of charge in the double layer can increase by applying a voltage between the metal and electrolyte. Commercially, EDLCs find used for energy storage, but they can also be used for sensing in at least several ways. For example, it can sense ions since the capacitance of the EDL is sensitive to concentration of ions.[128] Moreover, the double layer capacitance is also sensitive to temperature,[129] which has been used to create soft thermometers (albeit without the use of liquid metal). Finally, pressing liquid metal droplets encased in hydrogel will increase the surface area of the EDL capacitor, thereby driving current through an external circuit.

LMs are unique electrodes for EDLCs because the interfacial area increases with mechanical deformation, thus resulting in a variable area capacitor.[98] This change in capacitance can be used to drive charge through a circuit and thus convert mechanical energy into electricity (i.e., energy harvesting). It also can be used for sensing touch in which the sensor generates its own signal; such sensors are often called "self-powered" sensors. The output current of sensor is proportional to the change in the electrode area. Thus, it is possible to design sensors that detect body motion, such as the bending of a joint. EDLCs have a high capacitance in the range of tens of mF/m^2 due to the very small distances that separate the charges, as compared to classical capacitors that are separated by a solid dielectric layer and therefore have capacitances in the range of nF/m^2 to $\mu F/m^2$.[98] Consequently, variable EDLCs composed of LM in gel can be sensitive, although to date, the sensitivity has not been measured. EDLCs are also interesting because they interface electrical conductors (metal) such as those found in modern electronics with ionic conductors (electrolyte) such as those found in the body.

4.1.3. Resistive Transducer

LM conductors change resistance in response to deformation due to changes in the cross-section of the LM.[130,131] The gauge factor (GF) (also known as the sensitivity quantification transformer) is another measure of sensitivity expressed as the ratio of the relative change of the signal responses under the external strain loading. GF for resistive sensors can be calculated by Equation (3). R, ρ, and ϑ are the resistance, resistivity, and the Poisson's ratio, respectively.[132]

$$\mathrm{GF} = \frac{\frac{R_2 - R_1}{R_1}}{\epsilon} = (1 + 2\vartheta) + \frac{\frac{\rho_2 - \rho_1}{\rho_1}}{\epsilon} \tag{3}$$

Since resistivity is a material property, it should be constant for bulk LM. In principle, the theoretical GF is ≈2 assuming the poison ratio is 0.5, which is common for elastomers. This GF is relatively low compared to other types of strain sensors in which resistivity of the sensor changes with strain, but it is nevertheless sufficient to sense very small deformations by using a Wheatstone bridge. The working mechanism of a LM-based resistive pressure sensor was demonstrated by decreasing the cross-sectional area and therefore the increased electrical resistance. The pressure could be calculated by measuring the voltage difference between nodes A and B in a Wheatstone bridge circuit.[133] However, Equation 3 assumes uniform deformation across the LM conductor. By applying local pressure to LM wires, it is possible to localize the deformation to increase the sensitivity. In addition, it is possible to use LM particles in soft composites in which ρ_2 differs significantly from ρ_1, leading to enhanced GF. For example, mixing LM particles and Fe particles into silicone produces a composite that changes resistance by several orders of magnitude in response to low strains. This type of response is quite unusual in composites. Often deformation can cause particles in the composite to move apart, thereby increasing the resistance.[134] In contrast, these LM composites become more conductive, so they are called positive piezocondcuctive.[67] Piezoconductivity is thought to arise due to the elongation of the LM particles with the strain and the concomitant decrease in the gap between particles. Using Fe or other magnetic particles in such composites allows the particles to be aligned prior to curing the encasing elastomer, which can create an anisotropic response of the resistance to strain.

Liquid metals are appealing for resistive sensors because when they are encased in elastomer, they have very little hysteresis during strain cycling.[127] In comparison with other sensors such as capacitive, piezoelectric, and optical sensors, resistive sensors do not need complex manufacturing. Hence, these types of sensors have been widely used in physiological sensing areas.[17,135]

Liquid metals can be dispersed into solutions or polymer matrices as micro-droplets or nano-sized particles. LM particles dispersed in elastomer are called "liquid metal elastomers".[136] These particles can greatly enhance the electrical, dielectric, and thermal properties of LM elastomeric composites without stiffening the elastomer. These can be useful for sensing; for example, LM particles, combined with magnetically aligned magnetic particles, can become more (or less) conductive depending on how they are deformed.[67,137] This concept, which is called "piezoconductivity" (i.e., conductivity that responds to touch) is a unique

sensing mechanism of touch. Section 4.2 discusses sensing deformation via changes in resistance arising from changes to the geometry of liquid metal; instead, piezoconductivity changes the percolated pathways between particles for electrical conduction in response to deformation. Dispersing spike-shaped nickel micro-particles can improve sensitivity[138] while aligning the particles by a magnetic field can impart anisotropy in the response.[137]

4.1.4. Electrochemical Transducer

Electrochemical sensors measure current and voltage between electrodes in electrolyte to detect with high sensitivity the presence of species, such as bio-analytes, dissolved in the electrolyte. Typically, there is a working, counter, and reference electrode in an electrochemical cell. LM can be used as an electrode[139] or as a stretchable interconnect[140] for electrochemical sensors. The reactivity of LM and the presence of the native oxide complicates the use of LM relative to typical electrodes used for electrochemistry, such as Pt or C. However, there are some useful features. LM-based electrodes are stretchable, soft, injectable, and printable. Since the surface terminates with oxide, there are many functional groups that can bind to the hydroxyls at the surface.[141] This could be used, in principle, to attach ligands that could bind analytes from solution. The binding could be sensed by changes in interfacial capacitance measured by impedance. The protective oxide layer can be removed (reduced) easily by applying a reducing potential.[80] The ability to quickly reset the surface can help address surface fouling and contamination, which can adversely affect the accuracy and sensitivity of the sensor.

A significant consideration of using LM for electrochemistry is that it is inherently reactive. The reduction potential of Ga and In are ≈−0.56 and −0.34 V (versus the standard hydrogen electrode, SHE) respectively at room temperature. It reacts readily with oxygen and water to form gallium oxide species even in the absence of potential. It can also participate in redox chemistry, in which gallium oxidizes while reducing species from solution. Such properties have been utilized to develop LM-based electrodes to detect various heavy metal ions.[142] While this can be useful in some cases, such as reducing metal salts to metal via galvanic replacement reactions, it is a feature that must be considered when designing electrodes for sensitive electrochemical measurements since typically electrochemists prefer inert electrodes when sensing species from solution. In addition, the electrochemical oxidation and reduction of the surface of LM can significantly alter the effective interfacial tension.[79] This ability is useful for moving and manipulating liquid metals at sub-mm length scales, but has not be used for sensors. For additional information, the readers are directed to reviews on the electrochemistry of gallium.[143-146]

4.2. Optical LM Transducer

LM can also be used as a light-modulating material for optical sensing. LM nanoparticles show plasmonic features such as localized surface plasmon resonances (LSPR) predominantly in the UV wavelength range,[147] as well as plasmonic coupling behaviors with gold or silver nanostructures in the visible and NIR region of electromagnetic spectrum.[148,149] Such optical responses of LMs have been explored for sensing applications. For instance, geometric changes of LM particles arising from deformation can be monitored via changes in transmission.[150] Plasmon resonances can also enhance optical signals from molecules at the interface of the particles, as is the case in surface-enhanced infrared absorption (SEIRA) spectroscopy.[150] In general, LM particles are attractive for plasmonic applications because of the ease with which they can be produced by simple sonication of LM in solution, yet such an approach produces particles with a distribution of sizes, which makes it difficult to control size-dependent resonant properties. To address this issue, it is possible to form small (≈20 nm), monodisperse particles at elevated temperatures by reducing Ga salts.[151]

Bulk LM can also be used optically to sense strain. Thin, rigid films (such as a layer of silica) on elastomer will buckle when compressed, thereby forming a diffractive surface due to the periodicity of the buckles. LM can adhere to these surfaces and conform to the buckles. Thus, the diffraction grating becomes reflective and easier to see by eye. Consequently, straining it in plane (via compression) causes it to switch from being flat and mirror-like to colorful due to light diffraction.[152]

We include here a few other examples of ways light can interface with LM in a way that may be useful for sensing. For example, LM can also serve as a catalyst to drive photochemical reactions,[153] which could be an additional tool for biosensing if the reactions are chosen judiciously. Likewise, LM particles can absorb light to cause localized heating[154,155] (LM can also generate heat via Joule heating by passing electricity through LM wires). While heating is not a type of sensor by itself, it is nevertheless a useful tool, particularly in biological environment in which LM particles can locally deliver heat and reactive species (such as reactive oxygen) in response to light. Particles coated with carbon can absorb NIR light, which can pass through the skin; this concept has been used to create particles that change shape in response to light by converting from round LM droplets into highly oxidized GaOOH rods that can disrupt cancer cells.[156]

4.3. Magnetic LM Transducer

Although LM is not inherently magnetic (i.e., it is diamagnetic), it can be rendered magnetic by mixing magnetic particles such as iron into LM. Alternatively, it is possible to use magnetic fields to induce an electric current in the liquid metal, which in turn generates its own magnetic field.[157] This phenomenon is known as electromagnetic induction. The interaction between the external magnetic field and the magnetic field generated by the electric current in the liquid metal causes it to deform or change shape. By analyzing the changes in the physical properties of the liquid metal, such as its shape or electrical conductance due to the shape deformation, the sensor can detect the presence or intensity of a magnetic field.[157]

Coils (inductors) composed of LM have been used for sensing and for transmitting information or energy to sensors. For example, soft coils composed of LM in elastomer implanted in the body can receive and transmit energy and signals through the

skin, which may be useful for implantable biosensors.[158] Liquid metal has also been used for magnetoresistive sensing that utilizes the magnetoresistive effect, which is the change in electrical resistance of certain materials when subjected to an applied magnetic field.

The advantages and disadvantages of each LM-enabled sensing mechanism is summarized in **Table** 2.

5. Liquid Metal-Based Biosensor Applications

LM-based biosensors offer several advantages compared to traditional methods for monitoring human health. These sensors support detection modalities that exhibit exceptional sensitivity, enabling the detection of trace amounts of biomarkers for early disease diagnosis. Their flexibility and easy integration into wearable and implantable devices facilitate continuous and real-time health monitoring, addressing limitations of traditional tests that rely on intermittent sampling, require unportable instruments, and necessitate trained personnel. Moreover, LM biosensors are cost-effective and portable, reducing the dependency on specialized laboratory equipment and enabling POC testing. The LM surface can also support various biochemical modifications for specific biomolecule interactions, which render them versatile and indispensable tools in the realm of medical diagnostics. In this section, we summarize recent applications that use LM for human health monitoring. First, we focus on LM-based on-skin biosensors for monitoring joint movement, pulse, and heart rate. These types of sensors typically measure strain or pressure. Then we highlight examples of LM-based multifunctional biosensors that can sense more than one parameter. Finally, we summarize LM-based biosensors for the detection of molecular biomarkers. The aim of this section is not only to summarize the recent advances but also to address the current challenges to enhance the sensitivity, working range, and stability of these sensors to guide future studies.

5.1. On-Skin Physiological Monitoring

Many LM-based biosensing applications involve skin-mounted sensors that perform real-time physiological monitoring of body motion, heart rate, and respiratory rate. In the following, we describe various applications in this application space that use LM.

5.1.1. Body Motion

The ability to monitor joint and muscle movement continuously is useful for exercise physiology, rehabilitation training, and detecting motion disorders associated with chronic disease and neurological disorders. Furthermore, detecting touch is important for human-machine interfaces. LM-based sensors are widely applied in the literature for these applications (**Table** 3). The sensing of body motion is typically done using capacitive, resistive, and to a lesser extent, magnet, sensing mechanisms.

Capacitive sensors can measure motion-induced deformation with negligible energy consumption, ultrahigh sensitivity, and good stability.[178] For example, capacitive sensors can monitor cervical spondylosis by measuring the pressure contour resulting from rotation of the head (**Figure** 2a).[179] The use of an array of icicle-shaped LM electrodes improves the sensitivity by effectively making the dielectric layer softer. To increase the range of sensing, it is possible to use a bilayer structure for the dielectric in the capacitor. One layer uses a liquid metal elastomer foam (LMFE) based on LM particles dispersed in an elastomer foam,[121] which is soft and therefore sensitive to small pressures. The other layer in the bilayer LMFE (B-LMFE) has a larger Young's moduli, which only deforms at higher pressures. Combined, the B-LMFE can detect both small and large pressures based on the fact it requires small/large pressure to deform the first/second layer, respectively (Figure 2b).[180] LM-based capacitive pressure sensors can detect dyskinesia, known as abnormal, involuntary movements that can occur as a side effect of certain medications, demonstrated by an ultra-compressible sensor (Figure 2c).[181] Another approach to increase the sensitivity of capacitive sensors of deformation is to use LME-composites as the electrode because the LM can increase the dielectric constant while maintain a low modulus. These capacitors detect motion of finger joints for grasping objects and quantifying proximal interphalangeal (PIP) joint gesturing.[182] Smaller LM droplets (D = 1 μm) in the composites increase the sensor signal up to 190% in comparison with larger-size droplets (D = 80 μm). Capacitive strain sensor using LM electrodes and PDMS can detect hand motion and gesticulation when attached to the wrist and pollicis brevis muscle[183] (Figure 2d). In this work, a liquid metal patterned stretchable and soft capacitive sensor is introduced, with enhanced dielectric properties enabled by the dispersion of graphite nanofiber (GNF) fillers in a polydimethylsiloxane (PDMS) substrate. Capacitive sensors that can self-heal in response to damaged have been demonstrated. For example, a self-healable PDMS/multiwalled carbon nanotube (PDMS/MWCNT) elastomer embedded with gallium alloys as the electrodes form a capacitive strain sensor that could be attached to the throat to detect the small strain changes during speaking and also measure strain changes due to various types of body motions.[184]

Piezoresistive stretchable strain sensors with skin-like elasticity can detect strain by measuring the resistance changes owing to the mechanical deformation.[130] For example, they have been used for measuring knee bending and the pressure associated with footsteps (Figure 2e).[169] In this research, iron particles were chosen to enhance the conductivity of elastomer. When the elastomer and EGaIn are mixed, the EGaIn undergoes fragmentation, resulting in the formation of microdroplets that become embedded between neighboring iron particle chains. When local pressure is applied, the initially isolated EGaIn droplets rupture, creating conductive pathways. Piezoresistive sensors that use LM microchannels in silicone elastomer can detect strain for measuring the angle of hip, knee, and ankles for lower extremity biomechanics.[185,186] For real world applications of wearable sensors, a recent study introduced a wireless strain sensor featuring outstanding mechanical attributes, such as softness and tissue-like adaptability, created through a LM/CNTs hydrogel composite. It effectively monitored the movements of a surgeon, even detecting minute deformations at 0.25% strain, and played a crucial role in a successful minimally invasive Caesarean procedure for the conservation of endangered animals.[187]

Table 3. Performance of recent LM-based biosensors to monitor body motion. (LOD = Limit of Detection).

Mechanism	Encasing	Conductor	Sensitivity, LOD, Response time	Working Range	Application Notes
Capacitance	Ecoflex	EGaIn[121]	0.992 pF kPa^{-1}	N/A	1000+ cycle stability, human body movement monitoring with position detection
Capacitance	EVA copolymer	Ag nanoparticles, EGaIn[164]	N/A	0%–800% Strain	Stretchability up to 800% strain, 10 000 cycles stability, using as a touch sensor for fingers
Capacitance	Silicone membrane, PVA	EGaIn[165]	N/A	0–70 degree angle	Inertial sensor with a free-moving EGaIn droplet to record lower arm gestures, wireless readout, stretch up to 600%
Resistance	Platinum-cured Ecoflex	PET Silver, EGaIn[166]	(2–20) × 10^{-3} kPa^{-1}	2–400 kPa	Finger touch or footstep pressure detection, 7 days stability over 500 cycles in 19 to 45 °C range
Resistance	Ecoflex, PET	EGaIn[167]	0.05 kPa^{-1}	4–100kPa	2500 cycles stability, object grasping detection in finger, thumb, and palm region
Resistance	Dragon Skin	Galinstan[168]	LOD 0.05 N	0–1.17 N	Multidirectional finger force detection
Resistance	PDMS	EGaIn[169]	0.37 Pa^{-1}, 0.33 s (LOD 1.2 N)	0-6667 kPa	Convexed microdomes based on the LM droplet assisted amalgamation lithography knee bending and foot pressing monitoring with 1000 cycle stability
Resistance	poly(acrylamide-co-acrylic acid)/Zr^{4+} (P(AAm-co-AAc)/Zr^{4+}) hydrogel	EGaIn, nickel and silicon dioxide particles[104]	GF = 7.16, LOD (0.1%)	0%–400%	Detect finger rehabilitation training in different periods, throat, nape, wrist, elbow, ankle, knee, finger bending
Resistance	Gluten	EGaIn[170]	N/A	200%–600%	Adhered to the forefinger, wrist, knee, and forehead. self-healing property
Resistance	α-thioctic acid, butyl acrylate	EGaIn[171]	N/A	0%–450%	Wearable intelligent devices, including bionic electronic skin, rapid self-healing (5 min, 60 °C)
Resistance	Ecoflex, SiO_2 microspheres with an average diameter of 200 µm	EGaIn[172]	GF = 10.3	0%–300%	Open mouth, cough, fist, elbow bending, and finger bending monitoring.
Resistance	poly(vinyl alcohol) (PVA)	EGaIn[173]	N/A	35–165 degree	Monitoring the movement of elbow, wrist, finger, and knee, walking, and running
Resistance	Ecoflex[]	EGaIn[174]	GF = 4.91, 116 ms	0%–320%	Different states of the finger, neck, breathing chest, robot's joint motion detection
Resistance	Polyimide (PI) films	Ag nanowires, Cu (electrodes), EGaIn[175]	N/A	0%–120%	A self-healing hybrid conductor for e-skin for hand motion detecting
Resistance	Ecoflex	EGaIn[176]	GF = 4.95	0%–550%	Joints, fingers, and wrists movements detection
Magnetic	Silicone rubber	Copper, Galinstan[113]	N/A	Axial tensile (0–16 mm)	Measure the curvature of a finger and feedback on the position of an endoscope, 500 cycles stability, 72 h durability, work in 20–65 °C
Magnetic	Ecoflex	EGaIn[177]	0.26 µV kPa^{-1} (LOD 1950 Pa), 40 ms	0–10 kPa	Self-powered tactile sensors with 8000 cycle stability in the range of 15–80 °C for elbow swing and knee bending monitoring

5.1.2. Pulse, Heart Rate, and Blood Pressure Monitoring

To prevent heart disease and monitor the treatment progress in patients with cardiovascular diseases, it is essential to develop sensors that can continuously measure heart rate, pulse rate, and blood pressure with high durability, fidelity, and sensitivity for long-term on-skin wearing.[188] Several studies use LM for continuous heart rate measurement (**Table 4**).

ECG sensors are standard devices used by medical personnel for monitoring heart functions.[193,194] Recent efforts have focused on making such devices stretchable and wearable. For example, a portable photoplethysmography (PPG) technique can measure pulse using a self-healable and LM electrodes deposited selectively on Cu traces on a thin film of PDMS.[195] The sensor is skin mounted, and the electrical characteristics of the sensor are significantly influenced by changes in resistance in the stretchable liquid-metal wires. To ensure stable electrical performance in stretchable electronics, the fabrication process incorporates "S"-shaped liquid-metal wires instead of straight lines. By using this design approach, the impact of resistance change during stretching is mitigated, thus maintaining consistent electrical properties. Also, LM-based ECG sensors can monitor heart abnormalities during exercise by

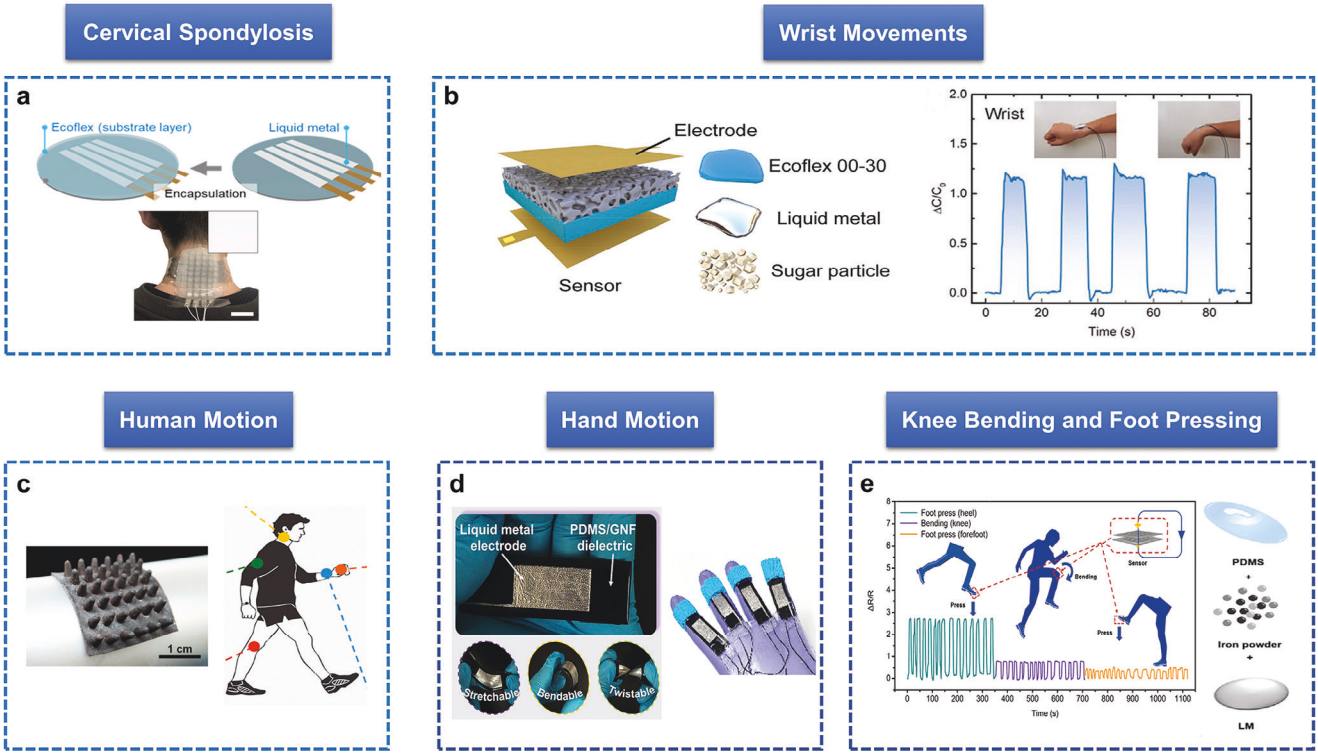

Figure 2. LM-based sensors for monitoring body motion. a) Schematic of encapsulating a liquid metal electrode cross-bar array in Ecoflex to place the capacitive sensor on the cervical region of the volunteer to obtain a pressure profile.[179] Copyright 2020, American Chemical Society. b) B-LMEF fabrication process and its applications as a wearable capacitance sensor for human motion detection.[180] Copyright 2022, Wiley-VCH GmbH. The bilayer design can detect both small and large pressure. c) LM elastomer-based capacitive stress sensor for human motion detection.[181] Copyright 2021, Elsevier. d) Capacitive strain sensor with liquid metal electrodes. Dielectric properties of the elastomer enhanced by the dispersion of graphite nanofiber (GNF) fillers in a polydimethylsiloxane (PDMS) substrate.[183] Copyright 2022, MDPI. e) Relative resistance changes of LM amalgams during foot pressing and bending of the knee.[169] Copyright 2021, Wiley-VCH GmbH.

using EGaIn as an electrode.[196,197] An integrated, flexible, and biocompatible ECG (electrocardiogram) chip-on-board was developed, featuring microfluidic LM interconnects and low-resistive carbon-black nanocomposite electrodes that contact the skin. The chip was designed to measure cardiovascular signals, specifically the inverting/non-inverting input (INP/INN) and body reference (GND), using low-power technology. The device has a Young's modulus two times less than PDMS only (**Figure 3a**).[198]

The pressure value required for sensing pulse varies from person to person and can also depend on factors such as age and physical activity. However, typically, a pressure range of ≈1.3 to 2.5 kPa is needed to detect the pulse using a wearable pressure sensor.[199] To meet the requirements for

Table 4. Performance of recent LM-based biosensors to monitor pulse rate, blood pressure, and breathe rate. For the working pressure range, some papers report force. Here, we have estimated pressure by normalizing by the size of the sensor. Ecoflex and Sylgard-184 are commercial silicones.

Mechanism	Encasing	Conductor	Sensitivity, LOD, Response time	Working Range	Characteristics
Magnetoelectric	Ecoflex	EGaIn[189]	16.88 mN, 1.01 ms	0–15 N (estimated as 0–10 kPa)	20 000 cycles stability, water resistant, pulse rate detection
Resistance	Sylgard-184	EGaIn[190]	68 N^{-1} (LOD 5 mN)	0–1000 mN (estimated as 0–2 kPa)	Arterial pulse waves and blood pressure monitoring with 500 cycle stability
Resistance	PVA, PLA	Galinstan[49]	0.158 kPa^{-1} (LOD 16 Pa)	0–600 kPa	Epidermal pulse rate, ECG, and cuffless blood pressure monitoring and stable over 4 weeks
Resistance	Graphene	EGaIn[191]	LOD 100 Pa	0–50 kPa	Real-time pulse monitoring, heart-rate monitoring, work in 20–50C, response time 90 ms
Electrochemical	Polyethylene terephthalate, Ecoflex	Galinstan[192]	2 kPa^{-1}, 50 ms (LOD 15 Pa)	0–0.22 kPa	10 000 cycles, wearable and artificial electronic skin devices, neck pulse and wrist pulse measurements

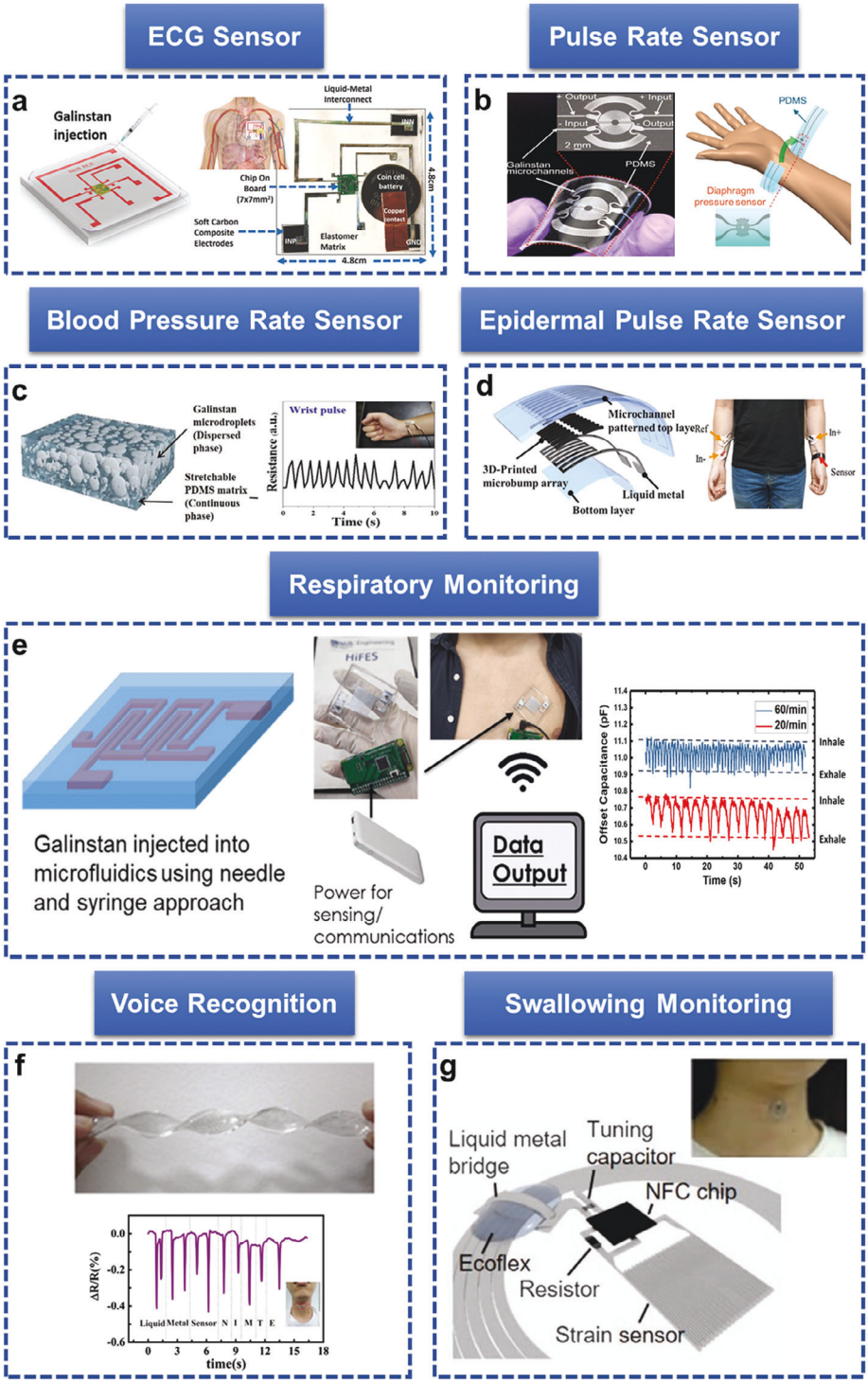

Figure 3. LM-based biosensors to monitor heart, pulse, blood pressure rate, respiratory, voice, and swallowing. a) Schematic of stretchable electrocardiogram (ECG) patch (SEP) and ECG monitoring analysis during exercise.[198] Copyright 2019, Wiley-VCH GmbH. The LM is used as interconnects. b) Microfluidic diaphragm pressure sensor for monitoring heart rate by changes in resistance through the LM Wheatstone bridge circuit.[191] Copyright 2017, Wiley-VCH GmbH. c) Liquid-metal-silicone composite (scale bar = 30 μm) for piezoresistive monitoring of pulse.[200] Copyright 2019, Elsevier. d) 3D-printed rigid microbump-integrated liquid metal-based pressure sensor (3D-BLiPS) under various forms of mechanical deformations and its application in epidermal pulse rate monitoring and cuffless blood pressure estimation.[49] Red (In^+) and white (Ref) electrodes were attached to the left arm and black (In-) electrodes were attached to the right arm. Copyright 2019, Wiley-VCH GmbH. e) A wireless LM-based respiratory tracker sensor with time dependence capacitance values.[202] Copyright 2019, MDPI. f) A highly stretchable LM-based strain sensor based on the resistivity changes mechanism for voice detection when the wearer speaks "Liquid," "Metal," "Sensor," and "NIMTE.[203] Copyright 2021, Wiley-VCH GmbH. g) Schematic illustration of the liquid-metal NFC device and its application in real-time wireless monitoring of swallowing.[204] Copyright 2017, Nature Portfolio.

these applications, a pressure sensor needs to measure in this pressure range with ultrahigh resolution and sensitivity (<50 Pa). To achieve this aim, a PDMS microfluidic diaphragm pressure sensor with LM microchannels embedded in a Wheatstone bridge circuit can provide the needed metrics (Figure 3b).[191]

Monitoring blood pressure requires detection of higher changes in pressure than that needed for pulse. It can also be challenging to measure pressure profile in various locations on curved and elastic surfaces. Soft LM elastomer (LME) can conform to such surfaces to detect blood pressure. Note that LME is inherently insulating, but becomes conductive after applying sufficient mechanical pressure to rupture the thin layers of elastomer that separate the particles (Figure 3c).[200] The sensors can detect epidermal pulse rate monitoring for cuffless blood pressure estimation to continuously monitoring of body pressure in specific areas prone to developing pressure ulcers, such as the sacrum, heel, ischium, ankle, and elbow, in order to prevent the occurrence of bedsores. The signal response of the sensor was enhanced by locally concentrating microchannel deformation with small hysteresis and integrating the rigid microbump array with LM embedded microchannels (Figure 3d).[49] The proposed sensor could measure the pulse transit time (PTT) and the blood pressure wirelessly.

5.1.3. Breath Rate, Swallow, and Voice Detection Monitoring

The ability to sense vibrations and movement along the neck and throat enables detection of speech and respiratory or swallowing disorders. LM-based devices can monitor these things,[201,202] (**Table 4**). For instance,[201] a compressible and stretchable magnetoelectric sensor composed of $Nd_2Fe_{14}B$ powders, silicone, and LM particles with an arch-shaped air gap enable respiratory monitoring. Exhaled/inhaled breath deform the sensor and thereby cause changes in magnetic flux (Through the change of the distance between the electrical/magnetic components caused by an external force). In addition,[202] interdigitated LM electrodes in silicone microchannels form a capacitor that can monitor respiration due to changes in capacitance between the electrodes with deformation (Figure 3e).

Likewise, an LM-based stretchable resistive strain sensor can monitor human voice when attached to the human throat. The sensor recognized different voice patterns when speaking "Liquid," "Metal," "Sensor," and "NIMTE" (Figure 3f).[203] Strain sensors can sense human swallowing and communicate the information with near-field-communication (NFC). The liquid EGaInSn-based strain sensor is attached to the throat to monitor the movements of the vocal cords. The variation in the output voltage (V_{Out}) corresponding to applied tensile and compressive strain during swallowing, revealing distinct waveforms characterized by two concave peaks, each corresponding to a different measurement (Figure 3g).[204] Therefore, these studies demonstrate the potential of LM-based sensors for noninvasive, miniaturized, and portable monitoring of breath rate, swallowing, and voice patterns. To monitor these parameters, we need to measure the expansion and contraction of the chest or abdomen during respiration, as well as the movements of the muscles, structures in the throat and esophagus, airflow, and muscle activity in the vocal folds and surrounding structures respectively.

These instances emphasize the transformative impact of LM on sensor technologies, particularly in the realm of continuous and conformal health monitoring. LM-based capacitive pressure sensors prove invaluable for continuous heart rate measurement and monitoring cardiovascular functions during exercise, showcasing LM's durability and sensitivity. Furthermore, LM-enabled piezoresistive stretchable strain sensors offer applications in biomechanics, including the detection of joint movements and angles, contributing to the advancement of flexible and wearable sensor technologies. Additionally, LM-based devices play a crucial role in health monitoring beyond cardiovascular parameters, demonstrating their capability in detecting breath rate, swallowing, and voice patterns. These innovations underscore LM's versatility in providing enhanced sensitivity, durability, and adaptability for a wide range of health monitoring applications.

5.1.4. Sweat Rate Monitoring

A sweat rate sensor is crucial for managing hydration, enhancing performance, preventing heat-related illnesses, and collecting valuable data for research. It provides insights into sweat production, enabling informed decisions on hydration and performance for individuals, athletes, trainers, and researchers.[205] LM can be used as electrodes for sweat analysis and volumetric rate monitoring as sweat passes through microfluidic systems. LM is attractive for microfluidics[65] because it can be injected to form electrodes that span from the bottom to the top of the microchannel walls.[206] Such electrodes can measure the speed and length of droplets flowing through microchannels similar to a Coulter counter.[207] A circular sweat chamber (2-mm diameter) on the tape collected the sweat from the volunteers. To speed up the sweat secretion rate, the volunteer pedaled the stationary cycle machine for 15 min to accelerate the sweat secretion rate. As droplets pass through the channels, the electrodes measure capacitance, resulting in a multi-plateau capacitance waveform; each plateau corresponds to the droplet position in the microchannel (**Figure 4a**). Droplets were formed due to the air pumping in the microchannel. The device measured the velocity of droplets up to 424 μm s^{-1}, and no less than 435 μm for the length, with an error percentage of <7.2% for length and <2.8% for speed, respectively. The LM sensor maintains very good performance even when the chip was bent to an angle of 96° (Figure 4b). The LM capacitive sensor can monitor sweat rate by taping the chip to the skin of a human (Figure 4c). The human body can produce anywhere from 0.5 to 1.5 liters of sweat per hour during intense physical activity. The area of the sweat collection was ≈3.14 mm^2. So, the rate of sweat secretion can be calculated out by dividing the droplet volume by the droplet generation which would be estimated 0.027 μl mm^{-2} min^{-1}. A computer recorded multi-plateau capacitive waveform as the sweat-in-air droplet passed through the sensing area[43] (Figure 4d). While there are several ways to measure sweat rate, the appeal of this approach is the ability to electronically measure the rate.

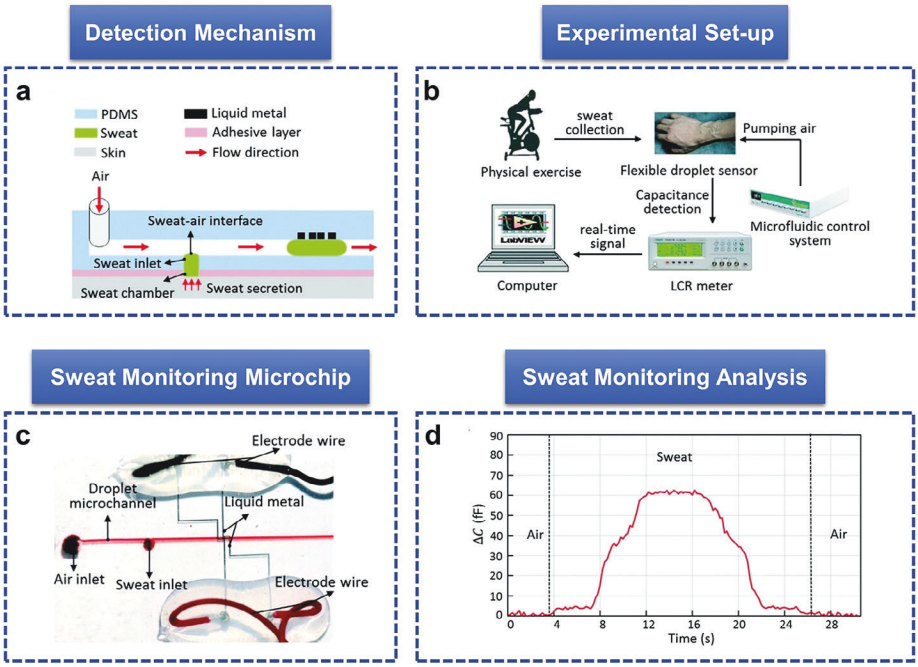

Figure 4. LM electrodes for sweat analysis.[43] a) Sweat droplet detection mechanism. b) The experimental set-up showing how sweat is collected. c) Sweat monitoring microchip. d) A multi-plateau capacitive waveform generated by a sweat-in-air droplet. Copyright 2020, The Royal Society of Chemistry.

5.1.5. Multifunctional Physiological Biosensors

Multifunctional sensors are needed to reduce the number of sensors placed on human body. Liquid metals are effective stretchable interconnects to connect different types of sensors[208–210] embedded in a skin-friendly soft elastomer (**Table 5**). Liquid metals can also be used as interconnects between sensors and power sources.[211,212] In addition, vertical liquid metal vias can connect liquid metal circuits vertically, resulting in a multi-layer integrated multi-sensor in which the bottom layer senses proximity/touch and the top layer senses pressure[213] (**Figure 5a**). LM vias connect the sensor layers. When a finger approached the proximity/touch sensor, the capacitance of the sensor changed as a function of distance change between the sensor and the finger. After touching the sensor, as pressure increased, the resistance of the pressure sensor also increased.

Systematically engineered circuits can also act as multifunctional sensors. For instance, double helix liquid metal fibers can sense torsion, strain, and touch via three mechanisms[118] (Figure 5b). First, twisting or stretching the coiled fibers changes the contact area between the fibers, resulting in an increase in capacitance between the fibers. Second, deformation from strain or twisting can cause an increase in resistance due to geometric changes to the fibers. Third, the fibers can sense touch due to self-capacitance between a finger and the fibers. Fibers filled with different amounts of liquid metal, such as filled one-third of the way, two-thirds of the way, and fully filled, can distinguish the location along the length where a user touches the bundle of twisted fibers.

Such hollow elastomeric fibers filled with liquid metal can monitor finger motion and bending movements through tribocharging. Touching the fibers produces a charge on the outside of the elastomeric fibers, which can be measured capacitively by the metal on the inside of the fibers. The multifunctional intrinsically stretchable liquid–metal fiber (ISLMF) (infused with EGaIn) can act as self-powered sensors for detecting motion. Unlike passive sensors that require continuous external signals for operation, the ISLMFs generate electric signals directly from motion. The contact forces applied to the ISLMFs affect the V_{oc} (open-circuit voltage) and I_{sc} (short-circuit current) outputs, which are shown to be dependent on the contact forces and effective contact area. The V_{oc} provides a stable response to static contact forces, while the I_{sc} exhibits instantaneous responses to contact and release of touching, making it suitable for detecting dynamic motion. The ISLMFs can be integrated into wearable interfaces, such as gloves, and used for various applications. For example, they can detect finger bending angles, convert touch into Morse code signals for transmission, and enable gesture recognition. The self-generating electric signals of the ISLMFs make them versatile and practical for wearable sensing applications. Thus, the fibers can detect nonverbal communication through touch created by a finger touch to communicate "SMART EGAIN FIBER", and numbers. Such stretchable liquid–metal fibers are multifunctional because they can also be used for energy harvesting using tribocharging or by harvesting electromagnetic waves from nearby electronic devices (Figure 5c).[214]

5.2. Detection of Molecular Biomarkers

LM-based biosensors have also been developed for detecting various biochemical species ranging from small gas molecules, ions,

Table 5. Performance of multi-functional and multi-application LM-based biosensors.

Mechanism	Sensor Types	Encasing	Conductor	Sensitivity, LOD, Response time	Working Range	Applications
Resistivity	Pressure, strain	Polyurethane fibers (PUF)	Galinstan[215]	GF = 1.55, 30 ms	0-30 MPa, 270%–600% strain	Underwater sensor with 10 000 cycles stability. Danger warning and hypothermia prevention at the same time and working in 46–116 C range
	Temperature, Strain	Dragonskin	EGaIn[209]	N/A	0–100 C, 0%–100% strain	Sensors, vibrators, and heaters are integrated in a single device as an all-in-one multimodal sensing and feedback system
	Multimodular strain (ECG, EMG)	PVA, Agarose	EGaIn[210]	N/A	0%–140% strain	Self-Healable Hydrogel—Liquid Metal Composite for heart rate monitoring
	Multifunctional strain	Ecoflex 00–30	ZnS, Ni, EGaIn[216]	N/A	0%–190% strain	Using five separate strain sensors to record and reconstruct human motion at elbow, knee, heel, and fingers with 200 cycles stability
	Acceleration, ECG, and temperature	(PET), CNT	Ag, EGaIn[208]	N/A	N/A	Detect temperature, acceleration, electrocardiograms, and environmental UV light under different states of physical activity, including walking, running, and sleeping.
	Strain, pressure, airflow	PVA	EGaIn[173]	1.2 Pa^{-1}, GF = 0.257	20–300 kPa	Monitoring the human movements such as elbow, wrist, finger, and knee, walking, and running with 200 cycles stability
Capacitance	Pressure, strain	3 M VHB tape	Galinstan[217]	10 ms	Bending test: 0–90 degree, Pressure test: 0–8 kg	Monitor human physiological signals, such as the motion angle of the wrist or finger joint and the pressure of fingers with 500 cycles stability
	Torsion, strain, tactile	SEBS Fiber	EGaIn [118]	LOD = 302 rad/m (torsion),2.9% (strain), 200 ms	0–10 800 rad m^{-1} (torsion), 0%–100% (strain)	Incorporating liquid metal into hollow elastomeric capillaries, fiber (200–800 µm) for finger touching detection
Capacitance, Resistivity	Pressure, tactile	PDMS	EGaIn[213]	N/A	0–300 kPa (Capacitance), 0–100 kPa (Resistivity), 0–20 cm (touch sensor)	Fingertip sensing for approaching, touching, and pressing detection.
Magnetoelec-tric	Strain, breath	Two-phase block copolymer PDMS and aliphatic isocyanate	Galinstan[218]	N/A	0%–560% (strain)	50 000 cyclic compression stability with self-powered and highly sensitive breathing monitoring application for the detection of early signs of breathing difficulties relevant to a variety of medical conditions in sleep pathologies or severe viral symptoms. Monitor finger-bending conditions.
	Multifunctional strain, tactile	Elastic poly(styrene-b-(ethylene-co-butylene)-b-styrene) (SEBS) hollow fiber	EGaIn[214]	N/A	0–120 degree finger bending angle	Self-powered sensors of motion and touch to detect finger bending angle, touch, and gestures.

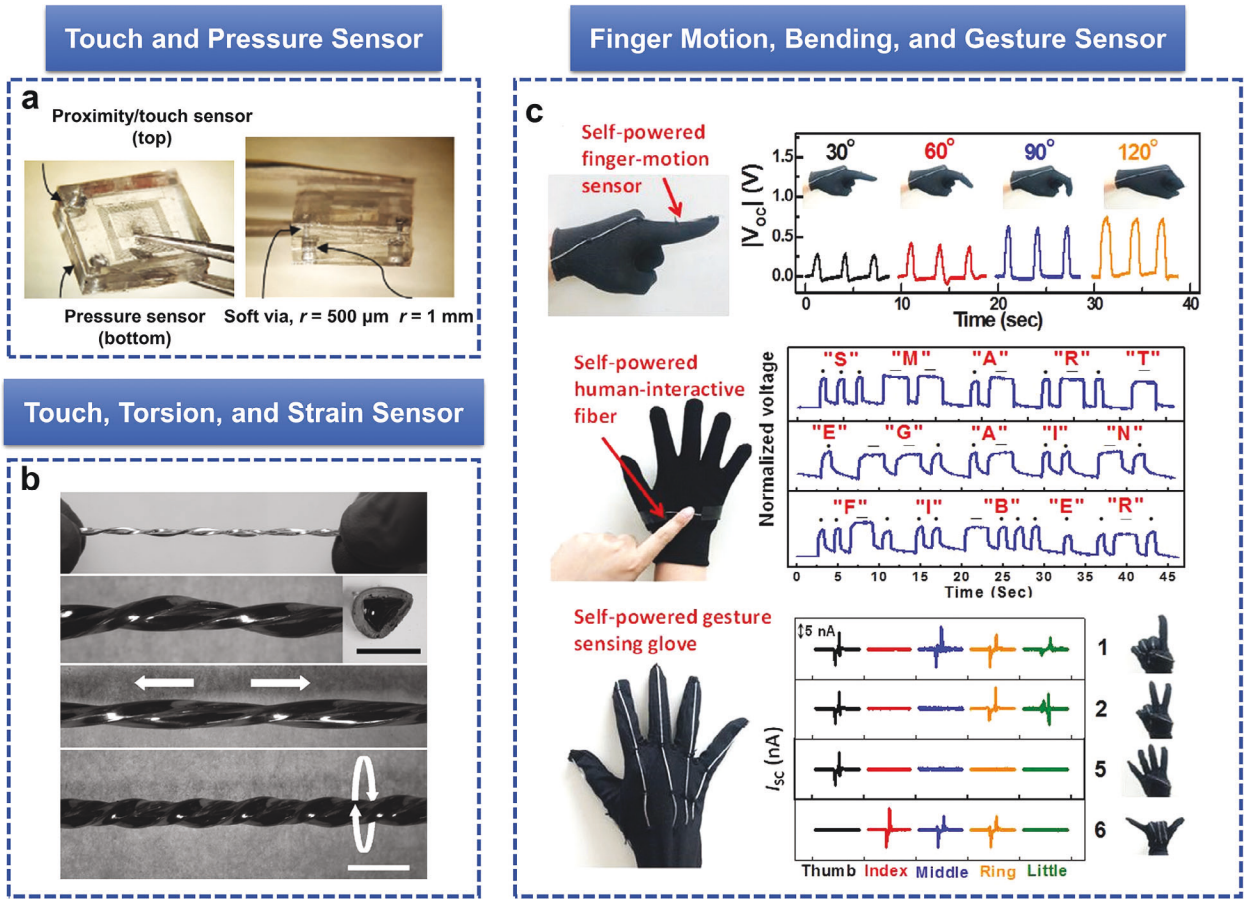

Figure 5. Multifunctional LM-based sensors. a) A two-layered sensor featuring a proximity/touch sensor and a pressure sensor (right) connected by soft LM vias (left).[213] Copyright 2018, Wiley-VCH GmbH. b) Photographs of double helix liquid metal fibers that can sense touch via changes in capacitance between fibers and a finger. They can also sense torsion by changes in capacitance between the fibers. Changes in resistance detect strain. From top to bottom: i) Twisted fibers. ii) The inset is the cross-section image of one fiber. iii) 150% elongated fiber. iv) Additionally twisted fibers.[118] Copyright 2017, Wiley-VCH GmbH. c) LM fibers for wearable self-powered sensing of finger motion, finger bending, and various gestures due to tribo-electrical signal generation by contacting/releasing between the intrinsically stretchable liquid–metal fiber skin.[214] Copyright 2021, Wiley-VCH GmbH.

and biomarker molecules such as glutamate and glucose. **Table 6** summarizes the recent studies in this field.

5.2.1. Gas Sensing

Gas sensors can find applications from environmental monitoring to disease diagnosis upon recognition of biomarker gas molecules released from infected human, animals, or plants.[32,219] Although researchers have explored LM predominately for sensing small-molecule gases (e.g., H_2, NO_2, NH_3, CO_2), LM-based gas sensing has the potential for the detection of more disease relevant VOC molecules. LM can sense gas due to its native oxide layer.[220] Microstructures of metal oxides can change their conductivity/resistance when they adsorbs gas molecules, thus enabling a measurable resistive response, which could be measured using two thin electrodes.[17] Typically, this is done at elevated temperatures. In addition, manipulating the size and morphology of sensing elements and incorporating a functional coating on LM layer can further tune the gas sensing interfaces, which allows LM to detect various gas successfully.[51,53]

For instance, a liquid metal oxide-based gas sensing device was demonstrated for detecting hydrogen (H_2) and nitrogen dioxide (NO_2) gases. Here, the H_2-sensing mechanism was based on the n-type behavior of Ga_2O_3. The number of free electrons on the sensor surface decreases due to the chemical interactions between oxygen ions on the sensor and H_2 gas molecules. This results in an increase in the resistance of sensing elements. Again, NO_2 can be detected through the chemisorption of gas molecules onto the sensor layer. The selectivity of the sensor can be achieved by the addition of other elements like In, Zn, or Sn into liquid Ga. While Ga-only based sensors can detect H_2 selectively above 300 °C, Ga-In based sensors detected NO_2 selectively at 150 °C with a LOD of 4.5 ppm.[51] Likewise, by casting a suspension of LM droplets across two copper electrodes, it is possible to form a resistive sensor that can detect NH_3 and NO_2 via physisorption. The resistance of the sensing element increases upon exposure to positively charged species (e.g., NH_3), and the resistance of the sensing element decreased when negatively charged species (e.g., NO_2) adsorb on the sensor surfaces (**Figure 6a**).[52] A film of LM

Table 6. Performance of LM-based biosensors for chemical and biomolecular target detection.

Mechanism	Sensor Types	Encasing	Conductor	Sensitivity, LOD, Response time	Working Range	Applications/Advantageous
Resistivity	Gas sensor	2D SnS_2 nanomaterials	EGaIn[54]	LOD = 1.32 ppb of NO	0–200 ppb of NO	Skin Compatibility, high responsiveness (1092%/ppm), early warning system for potential lung diseases
	Gas sensor	SiO_2/Si	Galinstan[52]	LOD = 1 ppm (NO_2), 20 ppm (NH_3)	0–12 ppm (NO_2), 0–100 ppm (NH_3)	Low temperature gas sensing
	Blood glucose sensor	PVC, Agarose	Bi, In, Sn[47]	N/A	5–50 mM glucose concentration	POC diagnostics, developed mobile phone platform, and real-time disease diagnostic
Capacitance	VOC gas sensor	PDMS	EGaIn[55]	3.37 (MeOH) 5.14 (EtOH) 6.59 (i-PrOH) (10^{-5}%/ppm)	0–75 000 ppm (MeOH), 0–35 000 ppm (EtOH), 0–25 000 ppm (i-PrOH)	Battery-free and wireless interrogation, bendable and twistable, soft and lightweight, and fast recovery time
Electrochemical	Sweat glucose sensor	PDMS	EGaIn[61]	LOD = 0.05 mM (Glucose), 15 mM (Na^+), and 8 mM (K^+)	0–1000 mM (Na^+, K^+)	Fast response time (30 s), non-invasive, wireless, and battery-free epidermal patch

NPs coated with polyaniline can form a shell for detecting HCl vapor. The LM-polyaniline composite provides a stable response compared to polyaniline alone. The improvement was due to the removal of insulating Ga oxide when the sensor was exposed to HCl. HCl dissolved the oxide layer, which results in an increment of electrical conductivity. Upon removal of the samples from the HCl vapor, the LM NPs underwent a spontaneous reformation of their native oxide layer in an oxidizing environment. This process facilitated the rapid recovery of the nanocomposite.[221] LM circuits can also detect hazardous CO_2. The sensor comprises an LM-based contact lens display (LM acted as interconnect for stretchable circuits), an air quality sensor, a microprocessor, and an eyeball camera. Here, LM acted as an interconnect for stretchable circuits and the air quality sensor detects the CO_2 concentration and sends the signal to the microprocessor., which illuminates the LED in the contact lens to green (CO_2<1000 ppm) or red (CO_2>4000 ppm) depending on the environmental CO_2 level (Figure 6b).[57]

For human health monitoring, a deformable epidermal sensor can analyze breathing. The sensor consists of LM nanoparticles on a filter membrane (formed by mechanical sintering) patterned on a PET substrate to form flexible electrodes. SnS_2 (which has strong affinity for NO gas, and molecular structure distortion of SnS_2 happens upon NO adsorption) was then drop-cast onto the LM electrodes to facilitate detection of NO gas, which is a biomarker for gaseous lung disorder.[54]

Volatile organic compounds (VOCs) are potential biomarkers for noninvasive detection of human and plant diseases[30,32,34,222]. LM electrodes in microfluidic channels function as an interdigitated capacitor that can sense changes in capacitance when VOCs absorb in the silicone dielectric between the LM electrodes. The platform involved the use of different solvents, namely isopropanol (with a relative permittivity, ϵ_r, of ≈18 at room temperature and 1 kHz probing frequency), ethanol ($\epsilon_r \approx 25$), and methanol ($\epsilon_r \approx 33$), which were directly in contact with the EGaIn electrodes. Since these alcohols possess varying relative permittivity values, their detection could be selectively achieved by measuring the capacitance while keeping the injected liquid volume constant (100 µL). The inductive coupling between a LM inductor and LM readout coil enabled the sensor to operate wirelessly and without the need for batteries. This all-soft sensing platform can detect methanol, ethanol, and isopropanol with LODs of 3.37, 5.14, and 6.59 ppm, respectively (Figure 6c).[55]

5.2.2. Nucleic Acid Detection

Several LM-based sensors have been demonstrated for DNA and microRNA (miRNA) detection. For example, [116] GaNPs deposited on Si can detect label-free DNA and single nucleotide polymorphism (**Figure** 7a). If the surface of the GaNP is functionalized with a 5′-end hexamethylthiol-modified DNA capture probe, it can bind specifically to the target DNA sequence (Figure 7b). The hybridization between the DNA capture probe and the target DNA sequence results in an energy shift of the inflection point around the RPH (reversal of polarization handedness) condition before and after successive modifications in the pseudodielectric function of the surrounding medium using ellipsometry (Figure 7c). This sensing approach takes advantage of the pseudodielectric function of the gallium plasmonic nanoparticles. This method allowed for sensitive and selective detection of the target DNA sequence with high accuracy.

In a recent study,[223] an innovative LM electrodynamic accumulation microfluidic (LEAM) device was introduced, showcasing its potential as a state-of-the-art technology for precise

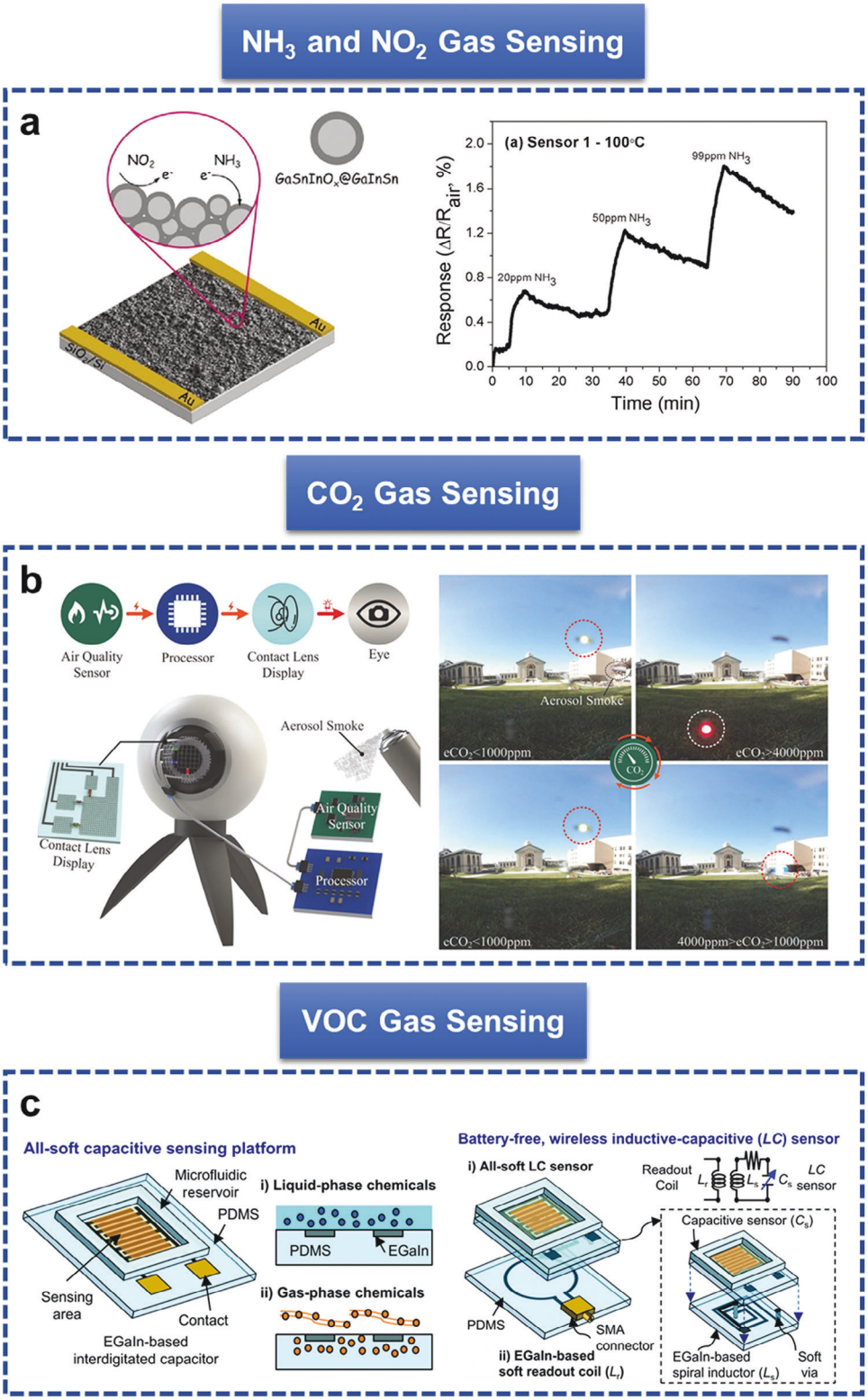

Figure 6. LM-based gas sensors. a) Schematic representation of casting a suspension of LM droplets across two copper electrodes to form a resistive sensor that can detect NH_3 and NO_2 via physisorption.[52] Copyright 2017, Elsevier. b) Schematic of air quality monitoring system (left) and response sequence of air quality based on the presence of CO_2 (right).[57] Copyright 2018, Wiley-VCH GmbH. c) All-soft microfluidic based VOC detection platform using EGaIn LM. Left: capacitive sensing platform; right: wireless inductive capacitive sensing platform.[55] Copyright 2017, The Royal Society of Chemistry.

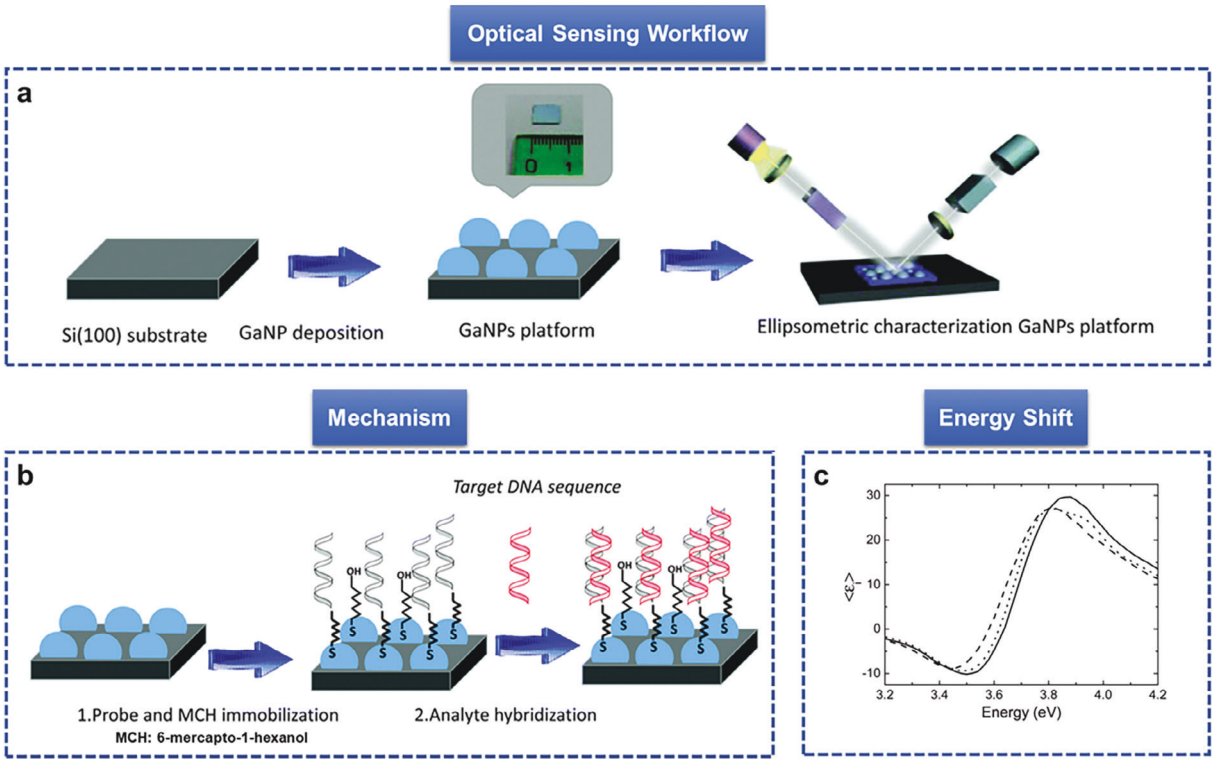

Figure 7. Representative example of LM-based optical biosensor for DNA sequence detection. a) Schematic representation of an optical biosensor based on GaNPs on Si for label-free DNA and single nucleotide polymorphism sensing.[116] b) Immobilization of the 5′-end hexamethylthiol DNA capture probe on the GaNP/Si platform and schematic representation of optical biosensor construction. c) Pseudodielectric spectra of a GaNP/Si platform before (black line) and after modification with HP1-SH (H. pylori, a single 12-mer sequence) (dotted line) and the probe/ 6-mercapto-1-hexanol (MCH) (dashed line). Copyright 2016, The Royal Society of Chemistry.

control of DNA by harnessing LM electrodes and an applied electric field (**Figure** 8a). The research methodology involved in-depth characterization of the distinctive properties exhibited by liquid metal when subjected to high voltages, enabling the meticulous management of DNA dynamics and thermodynamics (Figure 8b). DNA trapping involves capturing and immobilizing DNA molecules within a microfluidic device, enabling precise manipulation and analysis for various biotechnological applications (Figure 8c). The study employed a molecular beacon (MB) system with fluorescence-based detection to target microRNA (miRNA), which holds significant importance as a pivotal biomarker for a range of diseases, including nonalcoholic steatohepatitis (NASH) and Alzheimer's disease (AD). The outcomes underscore the successful and label-free detection of miRNA, highlighting the potential of electro-kinetic liquid biopsy systems for disease diagnosis and continuous disease progression monitoring (Figure 8d). This research presents a versatile and efficient approach for handling biomolecules and detecting specific gene molecules like miRNA in real-time.

5.2.3. Detection of Neurotransmitters

Flexible neural probes (electrodes) are useful to decrease the mechanical mismatch between the probes and soft neural tissues. However, soft and flexible probes deform or deflect during implantation into neural tissue. To overcome the current limitation, Ga was utilized to develop implantable probe that can turn from solid to liquid at body temperature and thus achieved temperature-dependent control of stiffness over five orders of magnitude. The compact ultra-large tunable stiffness (ULTS) probe also integrated Pt electrodes, microfluidic channels, and electrical interconnects all on a thin PDMS (30 μm) structure. The probes incorporated multilayer, deformable microfluidic channels for chemical agent delivery, electrical interconnects through Ga wires, and high-performance electrochemical glutamate sensing. Upon Ga melting, they became ultrasoft, flexible, and stretchable in all directions. The probe can be implanted 2 cm deep into agarose gel "brain phantoms" and rat brain under cooled conditions. Once inside the body, the body temperature melted Ga to form liquid metal wires, resulting in a flexible soft glutamate detecting sensor. The sensors detect glutamate electrochemically with a sensitivity of 8.2 ± 1.2 pA μM^{-1}, and a LOD of 0.39 ± 0.07 μM within ≈1 s response time[45] (**Figure** 9a). An in vitro selective dopamine sensing platform has also been demonstrated based on a reduced graphene oxide (rGO) on the surface of LM microdroplet system (LM-rGO). The LM–rGO composite proves effective as an electroactive modifier, reducing charge transfer resistance and enhancing sensing capabilities. Paper-based electrodes modified with LM–rGO showcased compatibility with low-cost commercial technologies.[224]

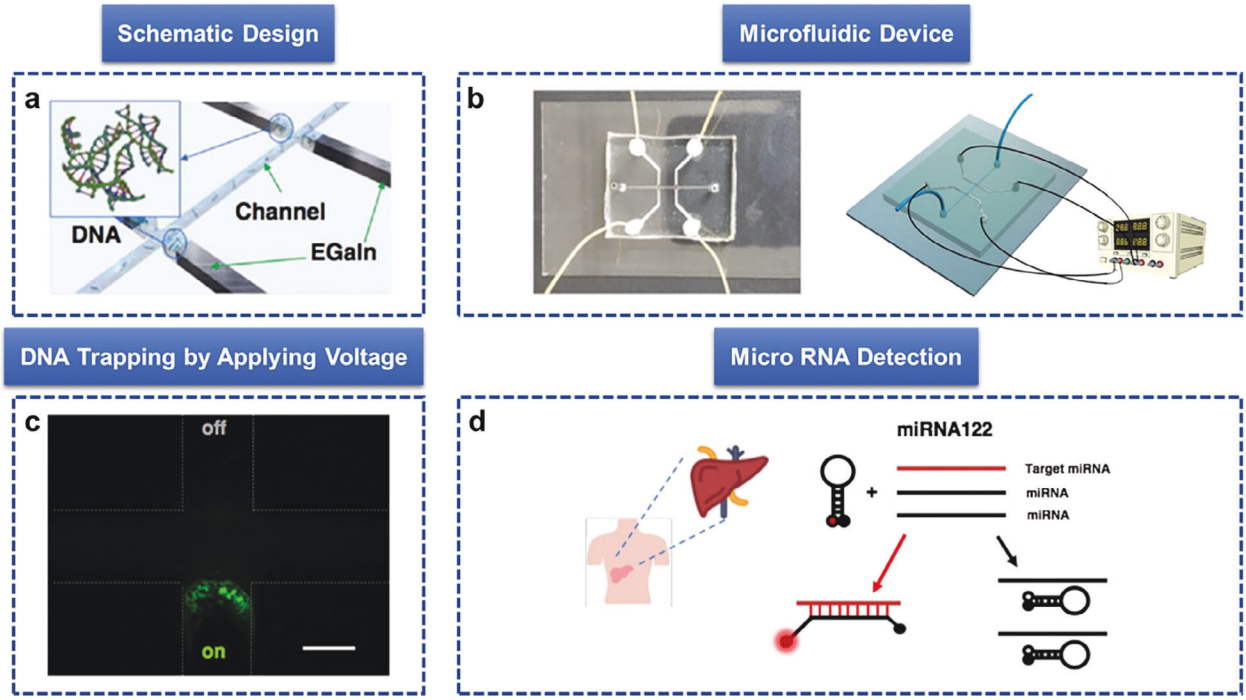

Figure 8. LM-based biosensor to trap DNA and detect miRNA.[223] a) DNA trapping schematic representation in the single main channel with the four EGaIn LM electrodes. b) Image of liquid metal electrodynamic accumulation microfluidic (LEAM) device. c) Trapping DNA on the turned-on LM electrode by applying 1 V. d) Schematic representation of Micro RNA 122 (miRNA) detection in the droplet LEAM system. Copyright 2023, Wiley-VCH GmbH.

5.2.4. Biomarker Analysis in Sweat and Blood

LM-based biosensors have also been used for detecting biomarkers such as glucose and exosomes in complex sample matrices. For example, LM antennas can combine with PDMS to create a liquid metal polymer conductor (LMPC) as a circuit and ion selective sensors (ISE) for detecting and analyzing metabolites (glucose), electrolytes (sodium ion (Na^+) and potassium ion (K^+)), and urea in sweat. Sweat sensing is attractive because it is a non-invasive way of measuring certain biomarkers of health. Although the LM itself does not serve as a sensor, the use of LM coils made it possible for the patch to be battery-free and remain soft. Battery free devices are attractive for a broad range of non-invasive diagnostic tools to monitor public health[61] (Figure 9b).

Blood glucose level quantification is now quite pervasive and also critical for chronic disease management such as diabetes. To facilitate blood glucose detection, a wireless electrochemical glucose detection platform was established that incorporated BIS [Bi (32.5 wt%), In (51 wt%), and Sn (16.5 wt%)] and a smartphone monitoring device together. Printing LM offers an excellent way for the rapid manufacture of electrodes. For data acquisition, a smartphone (Bluetooth feature) was used to help improve the portability and make the detection system suited to POC detection. With this sensing system, the concentration of glucose solution from 5 to 50 mM was analyzed[47] (Figure 9c).

The recently developed electrogenerated chemiluminescence (ECL) biosensor, incorporating g-C_3N_4-conjugated polydopamine-coated Galinstan liquid metal shell–core nanohybrids (g-C_3N_4@Galinstan-PDA) nanoprobes and a multivalent PAMAM-AuNPs electrode interface, has emerged as a highly sensitive tool for detecting multiple exosomes, recognized as biomarkers for various diseases (GPC_1, CD_9, CEA, and AFP), along with their surface proteins in real samples, including serum, urine, and blood.[115]

5.2.5. LM-Based Magnetic Biosensor for Red Blood Cell Counting

Blood hematocrit levels are important because they provide essential information about the oxygen-carrying capacity of the blood and can help diagnose and monitor various medical conditions. A 3D multilayer liquid-metal (Ga) microcoil can sense blood hematocrit level on a chip. The liquid metal microcoil serves as a receiver of a magnetic resonance relaxometry (MRR) measurement system in a lab-on-a-chip platform (Figure 9d). The blood is added to the chip. In a MRR measurement, the transverse relaxation rate of the blood sample increases quadratically with the hematocrit level due to higher magnetic susceptibility. Unlike commonly used centrifugation and optical method for determining blood hematocrit level, the microcoil composed of LM detects a subtle change in the blood hematocrit level by monitoring the transverse relaxation rate (R2). This portable MRR device is appealing for POC anemia diagnosis.[225]

5.3. Insertable Sensor for In Vivo Applications

Gastrointestinal (GI) dysmotility can lead to digestive conditions, which are associated with significant morbidity. The evaluation

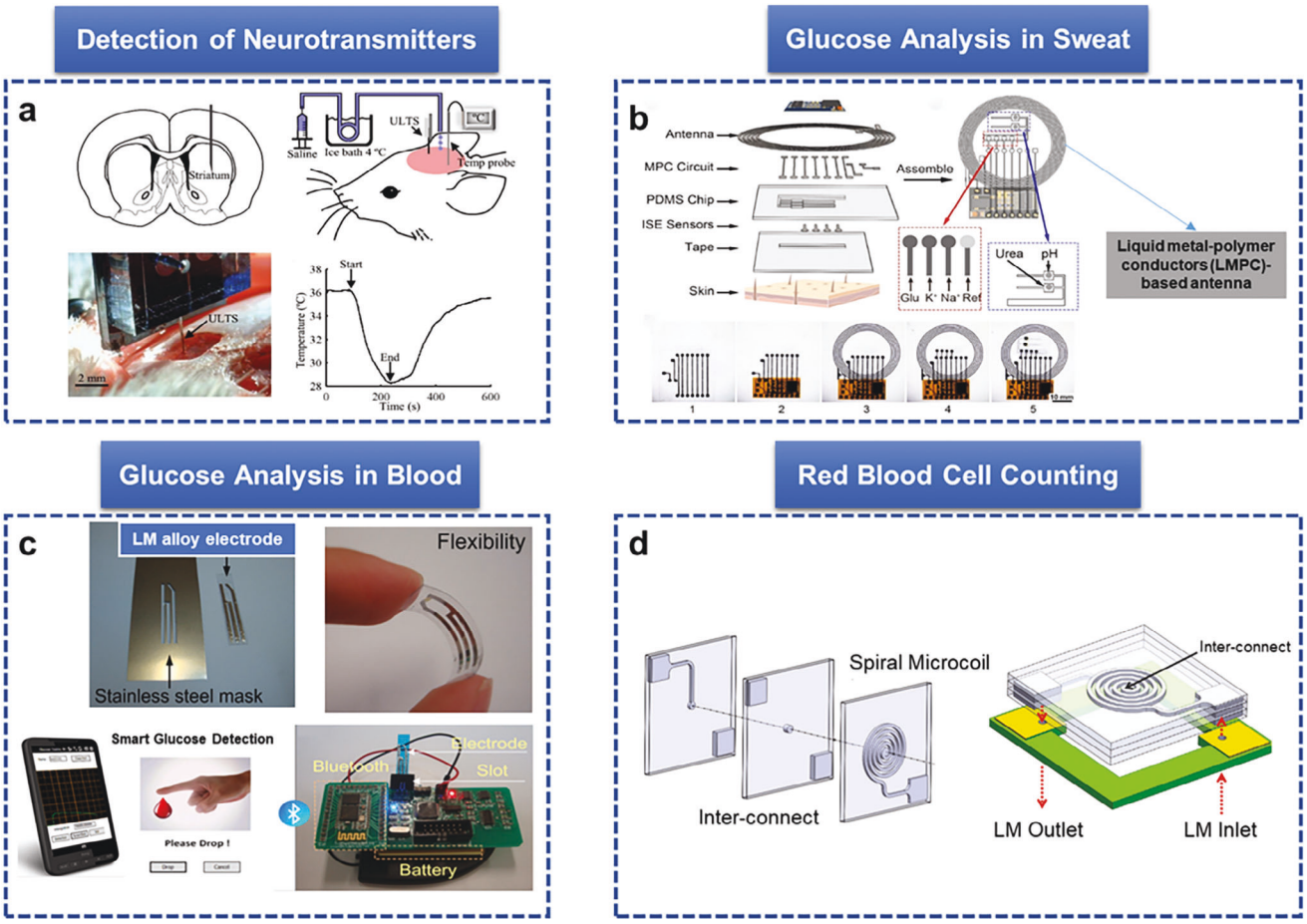

Figure 9. LM-based biochemical sensors. a) LM-based neural probe implanted in rats.[45] The metal is solid initially to facilitate implantation, but softens once it equilibrates with the body temperature. Copyright 2019, Elsevier. b) Wearable sweat sensor patch for noninvasive analyzing sweat metabolites and electrolytes using an antenna composed of a liquid metal-polymer conductors (LMPC).[61] Copyright 2022, Elsevier. c) A wireless blood glucose detection system integrated with smartphone and related hardware.[47] Copyright 2015, The American Society of Mechanical Engineers (ASME). d) Schematic representation of liquid-metal microcoils fabrication and liquid metal injection process as a magnetic biosensor to count the red blood cells.[225] Copyright 2015, Springer Science.

of patients with these symptoms involves multiple diagnostic elements, with manometry playing an important role. However, current manometry systems are limited by high cost, complexity, and bulkiness, which limit their use in less developed regions or non-hospital settings. Recently, a piezoresistive liquid metal-enabled pressure transducer (QUILT) system was developed for achieving desired pressure sensitivity across the dynamic range of the human GI tract. When an adequate amount of pressure was applied, the catheter infused with EGaIn experienced a reduction in cross-sectional area, leading to an elevation in the electrical resistance across the EGaIn material. This increase in resistance can be attributed to the piezoresistive effect. This low-cost, disposable, and portable device has potential for decentralization of GI-related healthcare and has been validated through in vitro tests and preliminary clinical utility in a porcine model.[226] QUILT offers simple and inexpensive fabrication procedures using basic bench tools such as syringes, scissors, and fast-drying silicone sealants. To fabricate QUILT, silicone tubing is trimmed, injected with EGaIn using a needle syringe, and copper wires are inserted into both ends to establish electrical connections. The ends are then sealed with fast-drying silicone sealant. Knots are tied at designated positions by hand or using a mechanical stretcher with designated tensile force and operate based on the resistivity change mechanism. To study the in vivo applications of the proposed sensor, two experiments were conducted. The first experiment evaluated the oesophageal pressure during the passage of an artificial food bolus attached to the tip of an endoscope. The second experiment evaluated the rectoanal pressure during rectoanal inhibitory reflex (RAIR) using a porcine model (Yorkshire swine, 40–80 kg weight). The results demonstrate that QUILT can extract real-time and spatially resolved information on GI motility under in vivo conditions for at least 2 hours, with a dynamic range consistent with human readings.

6. Challenges and Future Directions

Although liquid metals are promising candidates to fabricate various soft and wearable biosensors, there are a few limitations to be overcome in future biosensor development. First, although Ga is much less toxic than Hg, it is essential to thoroughly

characterize the toxicity and biocompatibility of Ga, in particular for long-term on-skin applications. Also, many sensing applications use nanoscale EGaIn particles. The toxicity profile of nanoscale LM materials may be different from their bulk counterparts. A safe packaging technology is needed to prevent possible LM leakage from the sensor device.[74] Second, the oxide layer of the surface of LMs is a double-sided sword. On one end, it can help stabilize LMs and improve the adhesion properties of LMs against different substrates. On the other end, the oxide layer on the surface of LM limits the ability to use LM for electrochemical sensing.[227] New concepts to use and manipulate the interface could help advance LM sensors.[228] Third, for biochemical sensing applications, it is essential to control the shape and size distribution of the liquid metal to optimize the sensitivity performance of the biosensor.[229] Patterning LM into nanoscale structures is still challenging. Fourthly, multifunctional LM biosensors face challenges in sensor integration and signal interference. It is essential to develop new fabrication methods and selective sensing materials or mechanisms that are specific to desired targets and biomarkers.

To date, researchers have primarily used geometric deformation of LM to sense mechanical inputs. Looking forward, there are many potential opportunities for innovative sensing approaches utilizing less explored properties of LMs such as the surface chemistry and optical characteristics. For example, the oxide layer has been used for sensing gases. In a different study, the use of Ga-based nanophotonic structures show surface-enhanced infrared absorption (SEIRA) spectroscopy to detect monolayer 1-octadecanethiol.[150] Moreover, integration of LMs in bioassays such as nucleic acid amplification assays or immune-sandwich assays would be an interesting future direction to enhance the assay performance and expand the biosensing application of LMs toward large biomolecules such as nucleic acids and proteins. Other anticipated advancements may include the inception of versatile soft wearable sensors capable of concurrently gauging diverse biophysical and biochemical parameters and analytes, heralding a transformative era of pliable and minimally invasive implantable sensing instruments for continuous in vivo monitoring. Additionally, the catalytic effects of Ga-based LMs are largely overlooked in sensing applications thus far, which may introduce opportunities for the formulation of soft catalytic sensors, especially in the context of enzyme-mimic activities. Durability and longevity are also in focus, ensuring these LM sensors can withstand harsh conditions while maintaining analytical performance. Finally, integration with wireless communication technologies enables the LM biosensors with real-time data transmission and analytics functions, while the flexible, stretchable forms promise comfort and versatility in wearable applications. As scholars venture into these unexplored domains, LMs are on the cusp of assuming a pivotal role in reshaping the biosensing landscape, offering enticing prospects for investigation, innovation, and transformative applications in the immediate future.

7. Conclusions

This review captures recent applications of liquid metals (mostly Ga and its alloys) in the biosensing area. To date, most of the Ga-based LMs biosensing applications involve on-skin wearable sensors to perform real-time physiological monitoring, such as tracking human body motions, heart and respiratory rates, voice and sweat secretion. LM-based biochemical sensing toward biomarker detection (e.g., VOC, neurotransmitter, and glucose) are also emerging, although they are much less reported compared to the physiological monitoring. Given LM's promising sensing performance that has been demonstrated so far, it is expected to continue to create many new opportunities in healthcare monitoring in the future.

Acknowledgements

The authors sincerely thank the funding support from the National Science Foundation (Award # 1944167).

Conflict of Interest

The authors declare no conflict of interest.

Keywords

biosensors, liquid metals, wearable sensors, soft materials, precision health, point-of-care

Received: July 15, 2023
Revised: December 25, 2023
Published online:

[1] W. R. Heineman, W. B. Jensen, *Biosens. Bioelectron.* **2006**, *21*, 1403.
[2] N. Bhalla, P. Jolly, N. Formisano, P. Estrela, *Essays Biochem* **2016**, *60*, 1.
[3] H. Yeon, H. Lee, Y. Kim, D. Lee, Y. Lee, J.-S. Lee, J. Shin, C. Choi, J.-H. Kang, J. M. Suh, H. Kim, H. S. Kum, J. Lee, D. Kim, K. Ko, B. S. Ma, P. Lin, S. Han, S. Kim, S.-H. Bae, T.-S. Kim, M.-C. Park, Y.-C. Joo, E. Kim, J. Han, J. Kim, *Sci. Adv.* **2021**, *7*, eabg8459.
[4] A. A. Tarar, U. Mohammad, S. K. Srivastava, *Biosensors (Basel)* **2020**, *10*, 56.
[5] M. Xu, D. Obodo, V. K. Yadavalli, *Biosens. Bioelectron.* **2019**, *124*, 96.
[6] S. Li, Y. Cong, J. Fu, *J. Mater. Chem. B* **2021**, *9*, 4423.
[7] D. C. Ferrier, K. C. Honeychurch, *Biosensors (Basel)* **2021**, *11*, 486.
[8] C.-M. Tîlmaciu, M. C. Morris, *Frontiers in Chemistry* **2015**, *3*.
[9] R. Guo, X. Wang, W. Yu, J. Tang, J. Liu, *Sci. China Technol. Sci.* **2018**, *61*, 1031.
[10] M. Song, X. Lin, Z. Peng, S. Xu, L. Jin, X. Zheng, H. Luo, *Frontiers in Materials* **2021**, *7*.
[11] T. Daeneke, K. Khoshmanesh, N. Mahmood, I. A. de Castro, D. Esrafilzadeh, S. J. Barrow, M. D. Dickey, K. Kalantar-zadeh, *Chem. Soc. Rev.* **2018**, *47*, 4073.
[12] M. Baharfar, K. Kalantar-Zadeh, *ACS Sens.* **2022**, *7*, 386.
[13] M. da C N Pinheiro, J. Luiz Martins do Nascimento, L. Carlos de Lima Silveira, J. Batista Teixeira da Rocha, M. Aschner, *Environmental Bioindicators* **2009**, *4*, 222.
[14] T. Cole, K. Khoshmanesh, S.-Y. Tang, *Advanced Intelligent Systems* **2021**, *3*, 2000275.
[15] Recent advancements in liquid metal enabled flexible and wearable biosensors, *Soft Science* **2023**, *3*, null.
[16] Y. Ren, X. Sun, J. Liu, *Micromachines* **2020**, *11*, 200.
[17] M. Zhang, X. Wang, Z. Huang, W. Rao, *Biosensors* **2020**, *10*, 170.
[18] L. Liu, H. Huang, X. Wang, P. He, J. Yang, *J. Phys. D: Appl. Phys.* **2022**, *55*, 283002.

[19] *Stimuli-Responsive Liquid Metal Hybrids for Human-Interactive Electronics – Kim – Advanced Functional Materials*, Wiley Online Library, USA.
[20] J. Ma, F. Krisnadi, M. H. Vong, M. Kong, O. M. Awartani, M. D. Dickey, *Adv. Mater. n/a*, 2205196.
[21] J. S. Gootenberg, O. O. Abudayyeh, J. W. Lee, P. Essletzbichler, A. J. Dy, J. Joung, V. Verdine, N. Donghia, N. M. Daringer, C. A. Freije, C. Myhrvold, R. P. Bhattacharyya, J. Livny, A. Regev, E. V. Koonin, D. T. Hung, P. C. Sabeti, J. J. Collins, F. Zhang, *Science* **2017**, *356*, 438.
[22] J. S. Chen, E. Ma, L. B. Harrington, M. Da Costa, X. Tian, J. M. Palefsky, J. A. Doudna, *Science* **2018**, *360*, 436.
[23] N. Mohammad, S. S. Katkam, Q. Wei, *The CRISPR Journal* **2022**.
[24] T. Yu, S. Zhang, R. Matei, W. Marx, C. L. Beisel, Q. Wei, *AIChE J.* **2021**, *67*, e17365.
[25] G. Bagdžiūnas, D. Palinauskas, *Biosensors* **2020**, *10*, 104.
[26] L. A. Stanciu, Q. Wei, A. K. Barui, N. Mohammad, *Annu. Rev. Biomed. Eng.* **2021**, *23*, 433.
[27] A. D. Nelson, P. Shiveshwarkar, B. Lim, G. Rojas, I. Abure, A. Shrestha, J. Jaworski, *Biosensors (Basel)* **2020**, *10*, 132.
[28] X. Jin, C. Liu, T. Xu, L. Su, X. Zhang, *Biosens. Bioelectron.* **2020**, *165*, 112412.
[29] Y. Y. Broza, R. Vishinkin, O. Barash, M. K. Nakhleh, H. Haick, *Chem. Soc. Rev.* **2018**, *47*, 4781.
[30] D. Tholl, O. Hossain, A. Weinhold, U. S. R. Röse, Q. Wei, *The Plant Journal* **2021**, *106*, 314.
[31] G. Silva, J. Tomlinson, N. Onkokesung, S. Sommer, L. Mrisho, J. Legg, I. P. Adams, Y. Gutierrez-Vazquez, T. P. Howard, A. Laverick, O. Hossain, Q. Wei, K. M. Gold, N. Boonham, *Emerg Top Life Sci* **2021**, *5*, 275.
[32] Z. Li, Y. Liu, O. Hossain, R. Paul, S. Yao, S. Wu, J. B. Ristaino, Y. Zhu, Q. Wei, *Matter* **2021**, *4*, 2553.
[33] A. D. Wilson, *Metabolites* **2015**, *5*, 140.
[34] G. Lee, O. Hossain, S. Jamalzadegan, Y. Liu, H. Wang, A. C. Saville, T. Shymanovich, R. Paul, D. Rotenberg, A. E. Whitfield, J. B. Ristaino, Y. Zhu, Q. Wei, *Sci. Adv.* **2023**, *9*, eade2232.
[35] J. S. Gootenberg, O. O. Abudayyeh, M. J. Kellner, J. Joung, J. J. Collins, F. Zhang, *Science* **2018**, *360*, 439.
[36] M. Hu, C. Yuan, T. Tian, X. Wang, J. Sun, E. Xiong, X. Zhou, *J. Am. Chem. Soc.* **2020**, *142*, 7506.
[37] Y. Dai, R. A. Somoza, L. Wang, J. F. Welter, Y. Li, A. I. Caplan, C. C. Liu, *Angew Chem Int Ed Engl* **2019**, *58*, 17399.
[38] N. Mohammad, S. S. Katkam, Q. Wei, *Angew. Chem.* **2022**, *134*, e202213920.
[39] H. Li, Y. Yang, J. Liu, *Appl. Phys. Lett.* **2012**, *101*, 073511.
[40] W. Zhang, C. Chen, D. Yang, G. Dong, S. Jia, B. Zhao, L. Yan, Q. Yao, A. Sunna, Y. Liu, *Adv. Mater. Interfaces* **2016**, *3*, 1600590.
[41] M. G. Mohammed, R. Kramer, *Adv. Mater.* **2017**, *29*, 1604965.
[42] S.-T. Han, H. Peng, Q. Sun, S. Venkatesh, K.-S. Chung, S. C. Lau, Y. Zhou, V. a. L. Roy, *Adv. Mater.* **2017**, *29*, 1700375.
[43] R. Zhang, Z. Ye, M. Gao, C. Gao, X. Zhang, L. Li, L. Gui, *Lab Chip* **2020**, *20*, 496.
[44] S.-Y. Tang, B. Ayan, N. Nama, Y. Bian, J. P. Lata, X. Guo, T. J. Huang, *Small* **2016**, *12*, 3861.
[45] X. Wen, B. Wang, S. Huang, T. "Leo" Liu, M.-S. Lee, P.-S. Chung, Y. T. Chow, I.-W. Huang, H. G. Monbouquette, N. T. Maidment, P.-Y. Chiou, *Biosens. Bioelectron.* **2019**, *131*, 37.
[46] Y. Jiao, C. Young, S. Yang, S. Oren, H. Ceylan, S. Kim, K. Gopalakrishnan, P. Taylor, L. Dong, *IEEE Sens. J.* **2016**.
[47] L. Yi, J. Li, C. Guo, L. Li, J. Liu, *Journal of Medical Devices* **2015**, *9*.
[48] X. Zhou, R. Zhang, L. Li, L. Zhang, B. Liu, Z. Deng, L. Wang, L. Gui, *Lab Chip* **2019**, *19*, 807.
[49] K. Kim, J. Choi, Y. Jeong, I. Cho, M. Kim, S. Kim, Y. Oh, I. Park, *Adv. Healthcare Mater.* **2019**, *8*, 1900978.
[50] T. Nakadegawa, H. Ishizuka, N. Miki, *Sens. Actuators, A* **2017**, *264*, 260.
[51] S. A. Idrus-Saidi, J. Tang, J. Yang, J. Han, T. Daeneke, A. P. O'Mullane, K. Kalantar-Zadeh, *ACS Sens.* **2020**, *5*, 1177.
[52] M. Shafiei, F. Hoshyargar, N. Motta, A. O'Mullane, *Materials and Design* **2017**, *122*, 288.
[53] W. Xie, F.-M. Allioux, R. Namivandi-Zangeneh, M. B. Ghasemian, J. Han, M.d. A. Rahim, J. Tang, J. Yang, M. Mousavi, M. Mayyas, Z. Cao, F. Centurion, M. J. Christoe, C. Zhang, Y. Wang, S. Merhebi, M. Baharfar, G. Ng, D. Esrafilzadeh, C. Boyer, K. Kalantar-Zadeh, *ACS Nano* **2021**, *15*, 16839.
[54] Y. Huang, F. Yang, S. Liu, R. Wang, J. Guo, X. Ma, *Research* **2021**, *2021*.
[55] M. Kim, H. Alrowais, C. Kim, P. Yeon, M. Ghovanloo, O. Brand, *Lab Chip* **2017**, *17*, 2323.
[56] M. Shafiei, N. Motta, F. Hoshyargar, A. P. O'Mullanc, **2015**.
[57] C. Pan, K. Kumar, J. Li, E. J. Markvicka, P. R. Herman, C. Majidi, *Adv. Mater.* **2018**, *30*, 1706937.
[58] M. M. Y. A. Alsaif, N. Pillai, S. Kuriakose, S. Walia, A. Jannat, K. Xu, T. Alkathiri, M. Mohiuddin, T. Daeneke, K. Kalantar-Zadeh, J. Z. Ou, A. Zavabeti, *ACS Appl. Nano Mater.* **2019**, *2*, 4665.
[59] M.d. A. Rahim, F. Centurion, J. Han, R. Abbasi, M. Mayyas, J. Sun, M. J. Christoe, D. Esrafilzadeh, F.-M. Allioux, M. B. Ghasemian, J. Yang, J. Tang, T. Daeneke, S. Mettu, J. Zhang, M. H. Uddin, R. Jalili, K. Kalantar-Zadeh, *Adv. Funct. Mater.* **2021**, *31*, 2007336.
[60] M. Chen, Z. Wang, Q. Zhang, Z. Wang, W. Liu, M. Chen, L. Wei, *Nat. Commun.* **2021**, *12*, 1416.
[61] L. Mou, Y. Xia, X. Jiang, *Biosens. Bioelectron.* **2022**, *197*, 113765.
[62] W. M. Haynes, D. R. Lide, T. J. Bruno, Eds., *CRC Handbook of Chemistry and Physics*, 97th ed., CRC Press, Boca Raton, **2016**.
[63] I. D. Joshipura, C. K. Nguyen, C. Quinn, J. Yang, D. H. Morales, E. Santiso, T. Daeneke, V. K. Truong, M. D. Dickey, *iScience* **2023**, *26*, 106493.
[64] S. Handschuh-Wang, T. Gan, M. Rauf, W. Yang, F. J. Stadler, X. Zhou, *Materialia* **2022**, *26*, 101642.
[65] K. Khoshmanesh, S.-Y. Tang, J. Y. Zhu, S. Schaefer, A. Mitchell, K. Kalantar-zadeh, M. D. Dickey, *Lab Chip* **2017**, *17*, 974.
[66] J. Tang, X. Zhao, J. Li, R. Guo, Y. Zhou, J. Liu, *ACS Appl. Mater. Interfaces* **2017**, *9*, 35977.
[67] G. Yun, S.-Y. Tang, S. Sun, D. Yuan, Q. Zhao, L. Deng, S. Yan, H. Du, M. D. Dickey, W. Li, *Nat. Commun.* **2019**, *10*, 1300.
[68] N. Kazem, M. D. Bartlett, C. Majidi, *Adv. Mater.* **2018**, *30*, 1706594.
[69] S. Chen, H.-Z. Wang, R.-Q. Zhao, W. Rao, J. Liu, *Matter* **2020**, *2*, 1446.
[70] M. D. Dickey, *Adv. Mater.* **2017**, *29*, 1606425.
[71] C. N. Cochran, L. M. Foster, *J. Electrochem. Soc.* **1962**, *109*, 144.
[72] T. W. Clarkson, L. Magos, *Crit. Rev. Toxicol.* **2006**, *36*, 609.
[73] R. Guo, X. Sun, S. Yao, M. Duan, H. Wang, J. Liu, Z. Deng, *Adv. Mater. Technol.* **2019**, *4*, 1900183.
[74] Y. Lu, Q. Hu, Y. Lin, D. B. Pacardo, C. Wang, W. Sun, F. S. Ligler, M. D. Dickey, Z. Gu, *Nat. Commun.* **2015**, *6*, 10066.
[75] C. R. Chitambar, *Int J Environ Res Public Health* **2010**, *7*, 2337.
[76] C. S. Ivanoff, A. E. Ivanoff, T. L. Hottel, *Food Chem. Toxicol.* **2012**, *50*, 212.
[77] J.-H. Kim, S. Kim, J.-H. So, K. Kim, H.-J. Koo, *ACS Appl. Mater. Interfaces* **2018**, *10*, 17448.
[78] T. Liu, P. Sen, C. J. Kim, *J. Microelectromech. Syst.* **2012**, *21*, 443.
[79] M. R. Khan, C. B. Eaker, E. F. Bowden, M. D. Dickey, *Proc Natl Acad Sci U S A* **2014**, *111*, 14047.
[80] M. R. Khan, C. Trlica, M. D. Dickey, *Adv. Funct. Mater.* **2015**, *25*, 671.
[81] K. B. Ozutemiz, J. Wissman, O. B. Ozdoganlar, C. Majidi, *Adv. Mater. Interfaces* **2018**, *5*, 1701596.
[82] H. Wang, B. Yuan, S. Liang, R. Guo, W. Rao, X. Wang, H. Chang, Y. Ding, J. Liu, L. Wang, *Mater. Horiz.* **2018**, *5*, 222.

[83] M. Pourbaix, *Second English Edition., National Association of Corrosion*, **1974**, Houston, Tex.
[84] M. R. Khan, C. Trlica, J.-H. So, M. Valeri, M. D. Dickey, *ACS Appl. Mater. Interfaces* **2014**, *6*, 22467.
[85] I. D. Joshipura, K. A. Persson, V. K. Truong, J.-H. Oh, M. Kong, M. H. Vong, C. Ni, M. Alsafatwi, D. P. Parekh, H. Zhao, M. D. Dickey, *Langmuir* **2021**, *37*, 10914.
[86] K. Kalantar-Zadeh, J. Tang, T. Daeneke, A. P. O'Mullane, L. A. Stewart, J. Liu, C. Majidi, R. S. Ruoff, P. S. Weiss, M. D. Dickey, *ACS Nano* **2019**, *13*, 7388.
[87] J. Ma, F. Krisnadi, M. H. Vong, M. Kong, O. M. Awartani, M. D. Dickey, *Adv. Mater.* **2023**, *35*, 2205196.
[88] Y.-G. Park, G.-Y. Lee, J. Jang, S. M. Yun, E. Kim, J.-U. Park, *Adv. Healthcare Mater.* **2021**, *10*, 2002280.
[89] M. D. Dickey, R. C. Chiechi, R. J. Larsen, E. A. Weiss, D. A. Weitz, G. M. Whitesides, *Adv. Funct. Mater.* **2008**, *18*, 1097.
[90] Y. Lin, O. Gordon, M. R. Khan, N. Vasquez, J. Genzer, M. D. Dickey, *Lab Chip* **2017**, *17*, 3043.
[91] S. Zhu, J.-H. So, R. Mays, S. Desai, W. R. Barnes, B. Pourdeyhimi, M. D. Dickey, *Adv. Funct. Mater.* **2013**, *23*, 2308.
[92] J.-H. So, J. Thelen, A. Qusba, G. J. Hayes, G. Lazzi, M. D. Dickey, *Adv. Funct. Mater.* **2009**, *19*, 3632.
[93] G. Li, X. Wu, D.-W. Lee, *Lab Chip* **2016**, *16*, 1366.
[94] E. Palleau, S. Reece, S. C. Desai, M. E. Smith, M. D. Dickey, *Adv. Mater.* **2013**, *25*, 1589.
[95] E. J. Markvicka, M. D. Bartlett, X. Huang, C. Majidi, *Nature Mater* **2018**, *17*, 618.
[96] J. Xu, Z. Wang, X. Wang, Y. Wu, R. Xing, T. Yu, Y. Li, J. Ao, Y. Tao, B. Bai, M. D. Dickey, D. Zhang, J. Yang, *Adv. Mater. Technol.* **2023**, *8*, 2201193.
[97] F. Suarez, D. P. Parekh, C. Ladd, D. Vashaee, M. D. Dickey, M. C. Öztürk, *Appl. Energy* **2017**, *202*, 736.
[98] V. Vallem, E. Roosa, T. Ledinh, W. Jung, T. Kim, S. Rashid-Nadimi, A. Kiani, M. D. Dickey, *Adv. Mater.* **2021**, *33*, 2103142.
[99] V. Vallem, Y. Sargolzaeiaval, M. Ozturk, Y.-C. Lai, M. D. Dickey, *Adv. Mater.* **2021**, *33*, 2004832.
[100] T. V. Neumann, M. D. Dickey, *Adv. Mater. Technol.* **2020**, *5*, 2000070.
[101] C. Ladd, J.-H. So, J. Muth, M. D. Dickey, *Adv. Mater.* **2013**, *25*, 5081.
[102] Y.-G. Park, H. Min, H. Kim, A. Zhexembekova, C. Y. Lee, J.-U. Park, *Nano Lett.* **2019**, *19*, 4866.
[103] Y.-G. Park, H. S. An, J.-Y. Kim, J.-U. Park, *Sci. Adv.* **2019**, *5*, eaaw2844.
[104] H. Wu, H. Qi, X. Wang, Y. Qiu, K. Shi, H. Zhang, Z. Zhang, W. Zhang, Y. Tian, *J. Mater. Chem. C* **2022**, *10*, 8206.
[105] J. Tang, J. Tang, M. Mayyas, M. B. Ghasemian, J. Sun, M. A. Rahim, J. Yang, J. Han, D. J. Lawes, R. Jalili, T. Daeneke, M. G. Saborio, Z. Cao, C. A. Echeverria, F.-M. Allioux, A. Zavabeti, J. Hamilton, V. Mitchell, A. P. O'Mullane, R. B. Kaner, D. Esrafilzadeh, M. D. Dickey, K. Kalantar-Zadeh, *Adv. Mater.* **2022**, *34*, 2105789.
[106] A. S. Algamili, M. H. Md Khir, J. O. Dennis, A. Y. Ahmed, S. S. Alabsi, S. S. Ba Hashwan, M. M. Junaid, *Nanoscale Res. Lett.* **2021**, *16*, 16.
[107] S. Yao, P. Swetha, Y. Zhu, *Adv. Healthcare Mater.* **2018**, *7*.
[108] Y. Yang, N. Sun, Z. Wen, P. Cheng, H. Zheng, H. Shao, Y. Xia, C. Chen, H. Lan, X. Xie, C. Zhou, J. Zhong, X. Sun, S.-T. Lee, *ACS Nano* **2018**, *12*, 2027.
[109] B. Zhang, L. Zhang, W. Deng, L. Jin, F. Chun, H. Pan, B. Gu, H. Zhang, Z. Lv, W. Yang, Z. L. Wang, *ACS Nano* **2017**, *11*, 7440.
[110] L. E. Helseth, *Nano Energy* **2018**, *50*, 266.
[111] C. Okutani, T. Yokota, H. Miyazako, T. Someya, *Adv. Mater. Technol.* **2022**, *7*, 2101657.
[112] H. An, L. Chen, X. Liu, X. Wang, Y. Liu, Z. Wu, B. Zhao, H. Zhang, *J. Micromech. Microeng.* **2021**, *31*, 035006.
[113] L.-Y. Zhou, Q. Gao, J.-F. Zhan, C.-Q. Xie, J.-Z. Fu, Y. He, *ACS Appl. Mater. Interfaces* **2018**, *10*, 23208.
[114] Y. He, L. Zhou, J. Zhan, Q. Gao, J. Fu, C. Xie, H. Zhao, Y. Liu, *3D Print. Addit. Manuf.* **2018**, *5*, 195.
[115] Y. Zhang, F. Wang, H. Zhang, H. Wang, Y. Liu, *Anal. Chem.* **2019**, *91*, 12100.
[116] A. G. Marín, T. García-Mendiola, C. N. Bernabeu, M. J. Hernández, J. Piqueras, J. L. Pau, F. Pariente, E. Lorenzo, *Nanoscale* **2016**, *8*, 9842.
[117] M. M. Y. A. Alsaif, F. Haque, T. Alkathiri, V. Krishnamurthi, S. Walia, Y. Hu, A. Jannat, M. Mohiuddin, K. Xu, M. W. Khan, Q. Ma, Y. Wang, N. Pillai, B. J. Murdoch, M. D. Dickey, B. Y. Zhang, J. Z. Ou, *Adv. Funct. Mater.* **2021**, *31*, 2106397.
[118] C. B. Cooper, K. Arutselvan, Y. Liu, D. Armstrong, Y. Lin, M. R. Khan, J. Genzer, M. D. Dickey, *Adv. Funct. Mater.* **2017**, *27*, 1605630.
[119] M. Weigel, T. Lu, G. Bailly, A. Oulasvirta, C. Majidi, J. Steimle, In **2015**, *Proceedings of the 33rd Annual ACM Conference on Human Factors in Computing Systems*, Association for Computing Machinery, New York, NY, USA, pp. 2991.
[120] Y.-F. Liu, Y.-Q. Li, P. Huang, N. Hu, S.-Y. Fu, *Adv. Electron. Mater.* **2018**, *4*, 1800353.
[121] J. Yang, D. Tang, J. Ao, T. Ghosh, T. V. Neumann, D. Zhang, Y. Piskarev, T. Yu, V. K. Truong, K. Xie, Y.-C. Lai, Y. Li, M. D. Dickey, *Adv. Funct. Mater.* **2020**, *30*, 2002611.
[122] R. Li, Q. Zhou, Y. Bi, S. Cao, X. Xia, A. Yang, S. Li, X. Xiao, *Sens. Actuators, A* **2021**, *321*, 112425.
[123] J. Zhou, A. Ellis, N. Voelcker, *Electrophoresis* **2010**, *31*, 2.
[124] D. Qi, K. Zhang, G. Tian, B. Jiang, Y. Huang, *Adv. Mater.* **2021**, *33*, 2003155.
[125] *Liquid Metal Interdigitated Capacitive Strain Sensor with Normal Stress Insensitivity – Zhang –2022 – Advanced Intelligent Systems*, – Wiley Online Library, -.
[126] S. Ali, D. Maddipatla, B. B. Narakathu, A. A. Chlaihawi, S. Emamian, F. Janabi, B. J. Bazuin, M. Z. Atashbar, *IEEE Sens. J.* **2019**, *19*, 97.
[127] H. Souri, H. Banerjee, A. Jusufi, N. Radacsi, A. A. Stokes, I. Park, M. Sitti, M. Amjadi, *Advanced Intelligent Systems* **2020**, *2*, 2000039.
[128] D. S. Silvester, R. Jamil, S. Doblinger, Y. Zhang, R. Atkin, H. Li, *J. Phys. Chem. C* **2021**, *125*, 13707.
[129] Temperature sensing using junctions between mobile ions and mobile electrons | PNAS.
[130] Nanomaterial-Enabled Wearable Sensors for Healthcare – Yao, **2018**. *Advanced Healthcare Materials*, – Wiley Online Library, -.
[131] Y.-L. Park, B.-R. Chen, R. J. Wood, *IEEE Sens. J.* **2012**, *12*, 2711.
[132] S. P. Beeby, G. Ensel, M. Kraft, *MEMS Mechanical Sensors*, illustrated edition., Artech Print on Demand, Boston, **2004**.
[133] T. Jung, S. Yang, *Sensors* **2015**, *15*, 11823.
[134] G. Yun, S.-Y. Tang, H. Lu, S. Zhang, M. D. Dickey, W. Li, *Small Science* **2021**, *1*, 2000080.
[135] F. Xu, X. Li, Y. Shi, L. Li, W. Wang, L. He, R. Liu, *Micromachines* **2018**, *9*, 580.
[136] N. Kazem, T. Hellebrekers, C. Majidi, *Adv. Mater.* **2017**, *29*, 1605985.
[137] G. Yun, S.-Y. Tang, Q. Zhao, Y. Zhang, H. Lu, D. Yuan, S. Sun, L. Deng, M. D. Dickey, W. Li, *Matter* **2020**, *3*, 824.
[138] G. Yun, S.-Y. Tang, H. Lu, T. Cole, S. Sun, J. Shu, J. Zheng, Q. Zhang, S. Zhang, M. D. Dickey, W. Li, *ACS Appl. Polym. Mater.* **2021**, *3*, 5302.
[139] P. Surmann, H. Zeyat, *Anal. Bioanal. Chem.* **2005**, *383*, 1009.
[140] X. Chen, H. Wan, R. Guo, X. Wang, Y. Wang, C. Jiao, K. Sun, L. Hu, *Microsyst. Nanoeng.* **2022**, *8*, 1.
[141] K. Y. Kwon, V. K. Truong, F. Krisnadi, S. Im, J. Ma, N. Mehrabian, T. Kim, M. D. Dickey, *Advanced Intelligent Systems* **2021**, *3*, 2000159.
[142] J. Zheng, M.d. A. Rahim, J. Tang, F.-M. Allioux, K. Kalantar-Zadeh, *Adv. Mater. Technol.* **2022**, *7*, 2100760.
[143] Y. Chung, C.-W. Lee, *J. Electrochem. Sci. Technol. 4*, https://doi.org/10.5229/JECST.2013.4.1.1.
[144] W. M. Saltman, N. H. Nachtrieb, *J. Electrochem. Soc.* **1953**, *100*, 126.
[145] M. Song, K. E. Daniels, A. Kiani, S. Rashid-Nadimi, M. D. Dickey, *Advanced Intelligent Systems* **2021**, *3*, 2100024.

[146] *Appl. Phys. Rev.*, | AIP Publishing, USA.
[147] P. Reineck, Y. Lin, B. C. Gibson, M. D. Dickey, A. D. Greentree, I. S. Maksymov, *Sci. Rep.* **2019**, *9*, 5345.
[148] Plasmonic properties of silver coated non-spherical gallium alloy nanoparticles | SpringerLink.
[149] I. D. Tevis, L. B. Newcomb, M. Thuo, *Langmuir* **2014**, *30*, 14308.
[150] X. Miao, T. S. Luk, P. Q. Liu, *Adv. Mater.* **2022**, *34*, 2107950.
[151] M. Yarema, M. Wörle, M. D. Rossell, R. Erni, R. Caputo, L. Protesescu, K. V. Kravchyk, D. N. Dirin, K. Lienau, F. von Rohr, A. Schilling, M. Nachtegaal, M. V. Kovalenko, *J. Am. Chem. Soc.* **2014**, *136*, 12422.
[152] M. G. Mohammed, M. D. Dickey, *Sens. Actuators, A* **2013**, *193*, 246.
[153] N. Syed, A. Zavabeti, M. Mohiuddin, B. Zhang, Y. Wang, R. S. Datta, P. Atkin, B. J. Carey, C. Tan, J. van Embden, A. S. R. Chesman, J. Z. Ou, T. Daeneke, K. Kalantar-zadeh, *Adv. Funct. Mater.* **2017**, *27*, 1702295.
[154] A. Heinzel, W. Hering, J. Konys, L. Marocco, K. Litfin, G. Müller, J. Pacio, C. Schroer, R. Stieglitz, L. Stoppel, A. Weisenburger, T. Wetzel, *Energy Technol.* **2017**, *5*, 1026.
[155] S. Wang, X. Zhao, J. Luo, L. Zhuang, D. Zou, *Composites, Part A* **2022**, *163*, 107216.
[156] Y. Lu, Y. Lin, Z. Chen, Q. Hu, Y. Liu, S. Yu, W. Gao, M. D. Dickey, Z. Gu, *Nano Lett.* **2017**, *17*, 2138.
[157] R. Guo, X. Sun, B. Yuan, H. Wang, J. Liu, *Adv. Sci.* **2019**, *6*, 1901478.
[158] A. Qusba, A. K. RamRakhyani, J.-H. So, G. J. Hayes, M. D. Dickey, G. Lazzi, *IEEE Sens. J.* **2014**, *14*, 1074.
[159] Y. Wang, G. Ma, Y. Zhang, L. Sheng, *Microsyst. Technol.* **2021**, *27*, 673.
[160] M. Kim, D. K. Brown, O. Brand, *Nat. Commun.* **2020**, *11*, 1002.
[161] S. Zhao, Y. Zhou, L. Wei, L. Chen, *Anal. Chim. Acta* **2020**, *1126*, 91.
[162] T. Hu, S. Xuan, L. Ding, X. Gong, *Sens. Actuators, B* **2020**, *314*, 128095.
[163] B. Ma, C. Xu, J. Chi, J. Chen, C. Zhao, H. Liu, *Adv. Funct. Mater.* **2019**, *29*, 1901370.
[164] J. Wang, G. Cai, S. Li, D. Gao, J. Xiong, P. S. Lee, *Adv. Mater.* **2018**, *30*, 1706157.
[165] M. Varga, C. Ladd, S. Ma, J. Holbery, G. Tröster, *Lab Chip* **2017**, *17*, 3272.
[166] J. C. Yeo, J. Y. Kenry, K. P. Loh, Z. Wang, C. T. Lim, *ACS Sens.* **2016**, *1*, 543.
[167] J. C. Yeo, J. Yu, Z. M. Koh, Z. Wang, C. T. Lim, *Lab Chip* **2016**, *16*, 3244.
[168] K. Kim, J. Ahn, Y. Jeong, J. Choi, O. Gul, I. Park, *Micro and Nano Systems Letters* **2021**, *9*, 2.
[169] W. Hu, Y. Li, S.-Y. Tang, L. Li, Q. J. Niu, S. Yan, *Adv. Mater. Interfaces* **2021**, *8*, 2100038.
[170] B. Chen, Y. Cao, Q. Li, Z. Yan, R. Liu, Y. Zhao, X. Zhang, M. Wu, Y. Qin, C. Sun, W. Yao, Z. Cao, P. M. Ajayan, M. O. L. Chee, P. Dong, Z. Li, J. Shen, M. Ye, *Nat. Commun.* **2022**, *13*, 1206.
[171] X. Wang, M. Zhao, L. Zhang, K. Li, D. Wang, L. Zhang, A. Zhang, Y. Xu, *Chem. Eng. J.* **2022**, *431*, 133965.
[172] S. L. Wang, X. Xu, Z. Han, H. Li, Q. Wang, B. Yao, *Mater. Lett.* **2022**, *308*, 131277.
[173] J. Xu, H. Guo, H. Ding, Q. Wang, Z. Tang, Z. Li, G. Sun, *ACS Appl. Mater. Interfaces* **2021**, *13*, 7443.
[174] J. Chen, J. Zhang, Z. Luo, J. Zhang, L. Li, Y. Su, X. Gao, Y. Li, W. Tang, C. Cao, Q. Liu, L. Wang, H. Li, *ACS Appl. Mater. Interfaces* **2020**, *12*, 22200.
[175] Y. Sohn, K. Chu, *Mater. Lett.* **2020**, *265*, 127223.
[176] Q. Gao, H. Li, J. Zhang, Z. Xie, J. Zhang, L. Wang, *Sci. Rep.* **2019**, *9*, 5908.
[177] X. Zhang, J. Ai, Z. Ma, Y. Yin, R. Zou, B. Su, *Adv. Funct. Mater.* **2020**, *30*, 2003680.
[178] *25th Anniversary Article: The Evolution of Electronic Skin (E-Skin): A Brief History, Design Considerations, and Recent Progress – Hammock –2013 – Advanced Materials*, Wiley Online Library, USA.
[179] Y. Zhang, S. Liu, Y. Miao, H. Yang, X. Chen, X. Xiao, Z. Jiang, X. Chen, B. Nie, J. Liu, *ACS Appl. Mater. Interfaces* **2020**, *12*, 27961.
[180] J. Yang, K. Y. Kwon, S. Kanetkar, R. Xing, P. Nithyanandam, Y. Li, W. Jung, W. Gong, M. Tuman, Q. Shen, M. Wang, T. Ghosh, K. Chatterjee, X. Wang, D. Zhang, T. Kim, V. K. Truong, M. D. Dickey, *Adv. Mater. Technol.* **2022**, *7*, 2101074.
[181] D. Zhang, Y. Zhong, Y. Wu, X. Zhang, M. D. Dickey, J. Yang, *Compos. Sci. Technol.* **2021**, *216*, 109066.
[182] Liquid Metal–Elastomer Soft Composites with Independently Controllable and Highly Tunable Droplet Size and Volume Loading | ACS Applied Materials & Interfaces.
[183] P. Bhuyan, D. Cho, M. Choe, S. Lee, S. Park, *Polymers (Basel)* **2022**, *14*, 710.
[184] X. Chen, P. Sun, H. Tian, X. Li, C. Wang, J. Duan, Y. Luo, S. Li, X. Chen, J. Shao, *J. Mater. Chem. C* **2022**, *10*, 1039.
[185] Y. Mengüç, Y.-L. Park, E. Martinez-Villalpando, P. Aubin, M. Zisook, L. Stirling, R. J. Wood, C. J. Walsh, In 2013 IEEE International Conference on Robotics and Automation, **2013**, pp. 5309.
[186] Y. Mengüç, Y.-L. Park, H. Pei, D. Vogt, P. M. Aubin, E. Winchell, L. Fluke, L. Stirling, R. J. Wood, C. J. Walsh, *Int. J. Robotics Research* **2014**, *33*, 1748.
[187] M. Sun, P. Li, H. Qin, N. Liu, H. Ma, Z. Zhang, J. Li, B. Lu, X. Pan, L. Wu, *Chem. Eng. J.* **2023**, *454*, 140459.
[188] A highly stretchable, transparent, and conductive polymer.
[189] X. Qu, J. Xue, Y. Liu, W. Rao, Z. Liu, Z. Li, *Nano Energy* **2022**, *98*, 107324.
[190] W. Xi, J. C. Yeo, L. Yu, S. Zhang, C. T. Lim, *Adv. Mater. Technol.* **2017**, *2*, 1700016.
[191] Y. Gao, H. Ota, E. W. Schaler, K. Chen, A. Zhao, W. Gao, H. M. Fahad, Y. Leng, A. Zheng, F. Xiong, C. Zhang, L.-C. Tai, P. Zhao, R. S. Fearing, A. Javey, *Adv. Mater.* **2017**, *29*, 1701985.
[192] H. Park, Y. R. Jeong, J. Yun, S. Y. Hong, S. Jin, S.-J. Lee, G. Zi, J. S. Ha, *ACS Nano* **2015**, *9*, 9974.
[193] G. Lu, F. Yang, J. A. Taylor, J. F. Stein, *J. Med. Eng. Technol.* **2009**, *33*, 634.
[194] M. M. Baig, H. Gholamhosseini, M. J. Connolly, *Med. Biol. Eng. Comput.* **2013**, *51*, 485.
[195] G. Li, D.-W. Lee, *Lab Chip* **2017**, *17*, 3415.
[196] J. S. Steinberg, N. Varma, I. Cygankiewicz, P. Aziz, P. Balsam, A. Baranchuk, D. J. Cantillon, P. Dilaveris, S. J. Dubner, N. El-Sherif, J. Krol, M. Kurpesa, M. T. L. Rovere, S. S. Lobodzinski, E. T. Locati, S. Mittal, B. Olshansky, E. Piotrowicz, L. Saxon, P. H. Stone, L. G. Tereshchenko, G. Turitto, N. J. Wimmer, R. L. Verrier, W. Zareba, R. Piotrowicz, *Heart Rhythm* **2017**.
[197] T. Shay, O. D. Velev, M. D. Dickey, *Soft Matter* **2018**, *14*, 3296.
[198] Y. Li, Y. Luo, S. Nayak, Z. Liu, O. Chichvarina, E. Zamburg, X. Zhang, Y. Liu, C. H. Heng, A. V.-Y. Thean, *Adv. Electron. Mater.* **2019**, *5*, 1800463.
[199] P.-H. Lin, W.-L. Chang, S.-C. Sheu, B.-R. Li, *iScience* **2020**, *23*, 101658.
[200] J. H. Oh, J. Y. Woo, S. Jo, C.-S. Han, *Sens. Actuators, A* **2019**, *299*, 111610.
[201] X. Zhang, J. Ai, R. Zou, B. Su, *ACS Appl. Mater. Interfaces* **2021**, *13*, 15727.
[202] Y. Li, S. Nayak, Y. Luo, Y. Liu, H. K. Salila Vijayalal Mohan, J. Pan, Z. Liu, C. H. Heng, A. V.-Y. Thean, *Materials (Basel)* **2019**, *12*, 1458.
[203] Y. Wu, Y. Zhou, W. Asghar, Y. Liu, F. Li, D. Sun, C. Hu, Z. Wu, J. Shang, Z. Yu, R.-W. Li, H. Yang, *Advanced Intelligent Systems* **2021**, *3*, 2000235.
[204] Y. R. Jeong, J. Kim, Z. Xie, Y. Xue, S. M. Won, G. Lee, S. W. Jin, S. Y. Hong, X. Feng, Y. Huang, J. A. Rogers, J. S. Ha, *NPG Asia Mater* **2017**, *9*, e443.

[205] L. B. Baker, *Sports Med* **2017**, *47*, 111.
[206] J.-H. So, M. D. Dickey, *Lab Chip* **2011**, *11*, 905.
[207] A. L. Richards, M. D. Dickey, A. S. Kennedy, G. D. Buckner, *J. Micromech. Microeng.* **2012**, *22*, 115012.
[208] Printed multifunctional flexible device with an integrated motion sensor for health care monitoring.
[209] J. Oh, S. Kim, S. Lee, S. Jeong, S. H. Ko, J. Bae, *Adv. Funct. Mater.* **2021**, *31*, 2007772.
[210] Self-Healable Hydrogel–Liquid Metal Composite Platform Enabled by a 3D Printed Stamp for a Multimodular Sensor System | ACS Applied Materials & Interfaces.
[211] D. Kim, D. Kim, H. Lee, Y. R. Jeong, S.-J. Lee, G. Yang, H. Kim, G. Lee, S. Jeon, G. Zi, J. Kim, J. S. Ha, *Adv. Mater.* **2016**, *28*, 748.
[212] S. Erlenbach, K. Mondal, J. Ma, T. V. Neumann, S. Ma, J. D. Holbery, M. D. Dickey, *ACS Appl. Mater. Interfaces* **2023**, *15*, 6005.
[213] M. Kim, H. Alrowais, O. Brand, *Adv. Electron. Mater.* **2018**, *4*, 1700434.
[214] Y.-C. Lai, H.-W. Lu, H.-M. Wu, D. Zhang, J. Yang, J. Ma, M. Shamsi, V. Vallem, M. D. Dickey, *Adv. Energy Mater.* **2021**, *11*, 2100411.
[215] X. Qi, H. Zhao, L. Wang, F. Sun, X. Ye, X. Zhang, M. Tian, L. Qu, *Chem. Eng. J.* **2022**, *437*, 135382.
[216] X. Wang, R. Guo, B. Yuan, Y. Yao, F. Wang, J. Liu, In **2018**, *2018 40th Annual International Conference of the IEEE Engineering in Medicine and Biology Society (EMBC)*, pp. 3276.
[217] L. Sheng, S. Teo, J. Liu, *J. Med. Biol. Eng.* **2016**, *36*, 265.
[218] C. Dong, A. Leber, T. D. Gupta, R. Chandran, M. Volpi, Y. Qu, T. Nguyen-Dang, N. Bartolomei, W. Yan, F. Sorin, *Nat. Commun.* **2020**, *11*, 3537.
[219] Z. Hetzler, Y. Wang, D. Krafft, S. Jamalzadegan, L. Overton, M. W. Kudenov, F. S. Ligler, Q. Wei, *Frontiers in Chemistry* **2022**, *10*.
[220] M. Ogita, K. Higo, Y. Nakanishi, Y. Hatanaka, *Appl. Surf. Sci.* **2001**, *175*, 721.
[221] C. Zhang, F.-M. Allioux, M.d. A. Rahim, J. Han, J. Tang, M. B. Ghasemian, S.-Y. Tang, M. Mayyas, T. Daeneke, P. Le-Clech, R. B. Kaner, D. Esrafilzadeh, K. Kalantar-Zadeh, *Chem. Mater.* **2020**, *32*, 4808.
[222] Z. Li, R. Paul, T. Ba Tis, A. C. Saville, J. C. Hansel, T. Yu, J. B. Ristaino, Q. Wei, *Nat. Plants* **2019**, *5*, 856.
[223] Y. Jeong, S. Noh, M. Yu, S. Chang, H. Eun, J. Kim, Y. Song, *Adv. Funct. Mater. n/a*, 2305680.
[224] M. Baharfar, M. Mayyas, M. Rahbar, F.-M. Allioux, J. Tang, Y. Wang, Z. Cao, F. Centurion, R. Jalili, G. Liu, K. Kalantar-Zadeh, *ACS Nano* **2021**, *15*, 19661.
[225] T. F. Kong, N.-T. Nguyen, *Microsyst Technol* **2015**, *21*, 519.
[226] K. Nan, S. Babaee, W. W. Chan, J. L. P. Kuosmanen, V. R. Feig, Y. Luo, S. S. Srinivasan, C. M. Patterson, A. M. Jebran, G. Traverso, *Nat. Biomed. Eng* **2022**, *6*, 1092.
[227] M. G. Saborio, S. Cai, J. Tang, M. B. Ghasemian, M. Mayyas, J. Han, M. J. Christoe, S. Peng, P. Koshy, D. Esrafilzadeh, R. Jalili, C. H. Wang, K. Kalantar-Zadeh, *Small* **2020**, *16*, 1903753.
[228] M. Song, M. D. Dickey, *Functional Organic Liquids*, John Wiley & Sons, Ltd, **2019**, pp. 251.
[229] X. Gao, X. Fan, J. Zhang, *Mater. Horiz.* **2021**, *8*, 3315.

Sina Jamalzadegan received his M.Sc. in Chemical Engineering from the University of Houston, Texas, USA in 2021. Currently, he is a Ph.D. candidate in Chemical Engineering at North Carolina State University, North Carolina, USA, under the supervision of Prof. Qingshan Wei. His research interests include point-of-care diagnostics, sensors, machine learning, artificial intelligence, biotechnology, and smart agriculture.

Sooyoung Kim is a Ph.D. candidate advised by Prof. Michael D. Dickey at North Carolina State University. His current research interests focus on the interfacial behavior of liquid metal and wearable pressure sensors.

Noor Mohammad completed his undergrad and masters from BUET in Bangladesh. He is currently a 5th year Ph.D. candidate at Wei lab at NC State University. His research focuses on the development of innovative CRISPR-based biosensing platforms. With a focus on creating a rapid, simple, sensitive, and cost-effective system, he aims to enable the detection of nucleic acid biomarkers, including viral genomes and cancer biomarkers, in point-of-care settings. By harnessing the power of CRISPR technology, he strives to make a significant impact in the field of molecular diagnostics.

Harshita Koduri received her M.Sc in Chemical Engineering along with a graduate certificate in Downstream Purification from North Carolina State University in 2022. She was a research assistant under the supervision of Prof. Qingshan Wei. Her research interests included point of care diagnostics, chip fabrication, and biotechnology. She is currently working for a pharmaceutical company based in North Carolina as a Manufacturing Sciences and Technology Engineer.

Zach Hetzler received his M.Sc. in Chemical Engineering from North Carolina State University in 2020. He is currently a Ph.D. candidate in Chemical & Biomolecular Engineering at North Carolina State University in Qingshan Wei's lab. His research interests include CRISPR diagnostics, sensor development, particularly for biomanufacturing and gene therapy as well as analytical chemistry, and point-of-care diagnostics.

Giwon Lee is an assistant professor in the Department of Chemical Engineering at Kwangwoon University. He received his B.S. in Chemical Engineering from Hanyang University in 2013 and Ph.D. in Chemical Engineering from Pohang University of Science and Technology in 2019. Then, he completed postdoctoral training in the Department of Chemical and Biomolecular Engineering at NC State before joining the faculty at Kwangwoon University. His research interests focus on developing stretchable/flexible electronics for various wearable human and plants applications.

Michael Dickey received a BS in Chemical Engineering from Georgia Institute of Technology (1999) and a PhD from the University of Texas (2006) under the guidance of Professor Grant Willson. From 2006-2008 he was a post-doctoral fellow in the lab of Professor George Whitesides at Harvard University. He is currently the Camille and Henry Dreyfus Professor in the Department of Chemical & Biomolecular Engineering at NCSU. He completed a sabbatical at Microsoft in 2016 and EPFL in 2023. Michael's research interests include soft matter (liquid metals, gels, polymers) for soft and stretchable devices (electronics, energy harvesters, textiles, and soft robotics).

Qingshan Wei is an associate professor in the Department of Chemical and Biomolecular Engineering at NC State. He is a member of the Emerging Plant Disease and Global Food Security Cluster and co-leads the Infectious Diseases focus area of the Global One Health Academy. He received his Ph.D. degree in Chemistry from Purdue University in 2012, and completed postdoctoral training in the Departments of Electrical Engineering and Bioengineering at UCLA between 2012-2016. His research interests focus on developing novel diagnostic assays and sensors for point-of-care detection of human and plant diseases.